



# DOPAS

(Contract Number: FP7 - 323273)

## Deliverable n° D3.21

### D3.21 Final results of EPSP laboratory testing

*Authors: Radek Vašíček, Lucie Hausmannová, Jiří Štáštka, Jiří Svoboda, Danuše Nádherná, Dana Pacovská, Jana Hubálovská, CTU in Prague; Petr Večerník, Dagmar Trpkošová, Jenny Gondolli, ÚJV Řež, a. s.; Markéta Dvořáková, Irena Hanusová, Lucie Bělíčková, SÚRAO;*

Date of issue of this report: **1/4/2016**

Start date of project: 01/09/2012

Duration: 48 Months

Project co-funded by the European Commission under the Euratom Research and Training Programme on Nuclear Energy within the Seventh Framework Programme		
Dissemination Level		
PU	Public	X
PP	Restricted to other programme participants (including Commission Services)	
RE	Restricted to a group specified by the partners of the DOPAS project	
CO	Confidential, only for partners of the DOPAS project	

Scope	Deliverable n°3.21	Version:	1.0
Type/No.	Report	Total pages:	71
		Appendices:	0
Title:	D3.21 Final results of EPSP laboratory testing	Articles:	5

#### ABSTRACT:

The aim of the DOPAS project is to address the design basis of, and reference designs and strategies for, plugs and seals to be used in geological disposal facilities. The Czech “Experimental Pressure and Sealing Plug” (EPSP) experiment is aimed at the study of developments concerning the design basis and reference designs. This report summarises the results of laboratory work related to the EPSP experiment. The laboratory research was undertaken as a supporting activity for the construction of the EPSP experiment. Various laboratory tests were performed on “Bentonit 75” selected as the principal material for the sealing part of the EPSP to verify its properties. Laboratory tests focused also on cement/concrete, grouting substances and rock samples parameters. Results of in-situ tests of the grouted rock massif around the EPSP experiment are also reported.

Laboratory testing provided input material parameters aimed at supporting the selection and confirming the quality of the delivered construction materials. A further data set was obtained for the purpose of the “verification testing” of the quality of the work carried out by the various subcontracting companies and to ensure that the relevant parameters concerning the various rock and concrete plug components were met in full. The final group of tests consisted of the study of small-scale physical models and the numerical analysis thereof as part of WP5.

The data was obtained during the period 2013-03/2016 under responsibility of the Czech DOPAS participants – the CTU in Prague, SÚRAO and ÚJV Řež, a. s.

#### RESPONSIBLE:

Centre of Experimental Geotechnics (CEG), Czech Technical University (CTU) in Prague, Radek Vašíček

#### REVIEW/OTHER COMMENTS:

Reviewed by SÚRAO, CTU and ÚJV, 31 March 2016

#### APPROVED FOR SUBMISSION:

Name: Johanna Hansen      Date: 31.8.2016

## Table of contents

1	Introduction .....	5
2	Qualitative requirements with respect to the EPSP construction materials.....	6
2.1	Bentonite seal .....	6
2.2	Concrete plugs .....	7
3	The laboratory testing plan.....	8
4	Results of laboratory tests .....	14
4.1	Work performed by the Centre of Experimental Geotechnics (CEG), CTU in Prague.....	14
4.1.1	Time schedule of the tests .....	14
4.1.2	Results of input laboratory tests on the bentonite.....	15
4.1.3	Thermo-physical properties.....	16
4.1.4	Comparison of B75_2013 with other Czech bentonites .....	17
4.1.5	Pellet manufacturing technology, quality verification and emplacement technology	19
4.1.5.1	Pellet production .....	19
4.1.5.2	Hydraulic conductivity and the swelling pressure of the pellets .....	21
4.1.5.3	Selection of the pellet mixture.....	22
4.1.5.4	Pellet emplacement tests at the “medium” scale .....	23
4.1.5.4.1	Emplacement of the pellet-ice mixture employing the Mixokret machine .....	24
4.1.5.4.2	Emplacement of pellets employing compaction plates .....	24
4.1.5.4.3	Emplacement of the pellet mixture using sprayed clay technology .....	25
4.1.5.4.4	Conclusions from the emplacement tests .....	25
4.1.5.5	Real application of bentonite pellets .....	28
4.1.6	Verification tests on concrete during and after installation.....	29
4.1.6.1	Requirements of the concrete plugs .....	29
4.1.6.2	Concrete composition.....	29
4.1.6.3	The testing of the fresh concrete – the settlement and flow table test.....	30
4.1.6.4	Uniaxial strength .....	30
4.1.6.5	Flexural strengths (first peak and ultimate).....	31
4.1.6.6	Hydraulic conductivity .....	32
4.1.6.7	pH leachate.....	33
4.1.6.8	Thermo-physical parameters .....	34
4.1.7	Conclusion regarding the work conducted by the CEG-CTU.....	35
4.2	Work performed by SÚRAO.....	36
4.2.1	Mineralogical composition of the bentonite.....	36
4.2.2	Filling of the fissures in the rock massif .....	36
4.2.3	In-situ tests .....	38
4.2.3.1	Water pressure tests of the rock mass .....	38
4.2.3.2	Goodman- Jack uniaxial press tests.....	42
4.2.4	Static plate test.....	42
4.2.5	Laboratory tests .....	43
4.2.6	Conclusion regarding the work conducted by the SÚRAO.....	43
4.3	Work performed by the ÚJV Řež, a. s.....	44
4.3.1	Laboratory tests on bentonite .....	44
4.3.1.1	Hydraulic conductivity tests.....	45
4.3.1.2	Gas permeability tests .....	47

4.3.2	Laboratory tests on grouting materials .....	48
4.3.3	Laboratory tests on the concrete/cement .....	49
4.3.3.1	pH measurements .....	49
4.3.3.2	Hydraulic conductivity .....	50
4.3.4	Laboratory tests on the host rock.....	50
4.3.4.1	Porosity .....	51
4.3.4.2	Hydraulic conductivity.....	51
4.3.5	Physical models.....	51
4.3.5.1	Physical hydraulic models.....	52
4.3.5.1.1	PHM with bentonite powder .....	53
4.3.5.1.2	PHM with bentonite pellets .....	56
4.3.5.2	Physical interaction models.....	58
4.3.5.2.1	Water content analysis of dismantled PIM.....	59
4.3.5.2.2	Trends in chemical composition of water sampled from PIM .....	61
4.3.5.2.3	Cation exchange capacity of selected bentonite samples .....	64
4.3.5.2.4	Specific surface area of selected bentonite samples .....	65
4.3.5.3	Concrete after PIM dismantling .....	65
4.3.6	Conclusion of the ÚJV's work .....	66
5	Conclusion.....	67
6	References .....	68
7	List of abbreviations.....	71

## 1 INTRODUCTION

The aim of the DOPAS project is to address the design basis of, and reference designs and strategies for, plugs and seals to be used in geological disposal facilities. The Czech “Experimental Pressure and Sealing Plug” (EPSP) experiment is engaged in the study of developments concerning the design basis and reference designs and strategies, including compliance issues.

Initially, laboratory testing provided input material parameters aimed at supporting the selection and confirming the quality of the delivered construction materials. A further data set was obtained for the purpose of the “verification testing” of the quality of the work carried out by the various subcontracting companies (rock permeability following rock improvement, strength parameters, concrete behaviour etc.) and to ensure that the relevant parameters concerning the various rock and concrete plug components were met in full. The final group of tests consisted of the study of small-scale physical models and the numerical analysis thereof as part of WP5.

This report presents the final laboratory results of the project finalized at the end of March 2016.

The data was obtained during the period 2013-03/2016 by the Czech DOPAS participants – the CTU in Prague, SÚRAO and ÚJV Řež, a. s. Verification tests were conducted principally by subcontractors engaged by SÚRAO (a tender for improvements to the experimental gallery, drilling and grouting) and the CTU (a tender for EPSP construction).

## 2 QUALITATIVE REQUIREMENTS WITH RESPECT TO THE EPSP CONSTRUCTION MATERIALS

The requirements of the materials to be used in the EPSP experiment were set out in the DOPAS Deliverable D2.1 Design Bases and Criteria report (White et. al., 2013). Figure 1 shows the various EPSP components and their construction materials. Glass fibre was used as the reinforcement material in the fibre shotcrete. The concrete blocks, which serve as a permeable “lost” or hidden formwork may, alternatively, be made of aerated concrete. More information is contained in D3.20: the EPSP plug test installation report (Svoboda et. al., 2016).

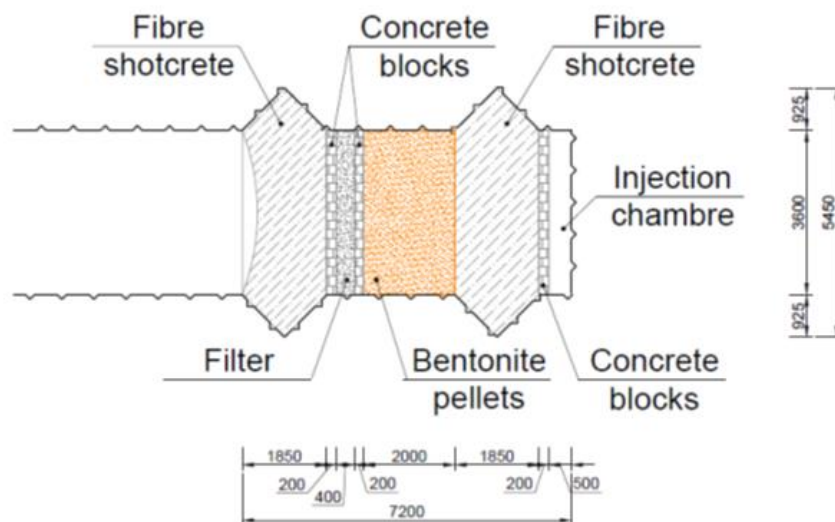


Figure 1 - Scheme of the conceptual design of the EPSP. Dimensions are in mm. (DOPAS Deliverable D2.1)

### 2.1 Bentonite seal

One of the main aims of the EPSP experiment consisted of the use of Czech materials and technologies. It is important to mention here that Czech deposits contain no Na-type bentonites. These requirements, together with requirements concerning the construction of the plug itself led to the determination of a set of selection criteria regarding the bentonite sealing material:

- Local material (CZ)
- Non-activated
- Fulfilment of the various sealing requirements (see deliverable D2.1, White et. al., 2013)
- Homogenous material
- Available in sufficient quantity
- Available in reasonable time

Following the careful consideration of plug construction requirements, factory-produced bentonite (milled, non-activated Ca-Mg bentonite) was selected as the principal material for the bentonite part of the plug. Commercially available “Bentonit 75” (B75) bentonite was found to be the only material readily available which fulfilled all the above criteria. Non-activated Ca-Mg Bentonit 75 bentonite is extracted from the Černý vrch deposit and is produced by Keramost, a. s.

The selection of B75 bentonite was supported by experience from previous research in which B75 was found to fully comply with requirements concerning hydraulic conductivity and swelling pressure (maximum  $10^{-12}$  m/s and 2MPa respectively at a dry density of  $1.4\text{g/cm}^3$ ).

It is well known that supplies of a natural material such as bentonite even supplied by the same producer may vary with respect to a number of parameters according to the area of the quarry in which the material

is extracted and the layer of the deposit. The B75 for the manufacturing of pellets and construction of the EPSP was delivered in 2013 (B75\_2013); the B75 previously tested was delivered in 2010. Therefore, the initial EPSP laboratory tests concentrated on determining a basic description of the material and the confirmation of its properties against the requirements set out in Deliverable D2.1 (White et. al., 2013).

## 2.2 Concrete plugs

Deliverable D2.1 also specifies requirements with concern to the concrete as follows:

- The strength of the concrete must be sufficient to withstand a maximum applied pressure of 7MPa.
- The construction of the concrete blocks walls of require concrete with reduced pH, the same as for the shotcrete. The pH value of the concrete has not yet been specified but is expected to be below 12.

More exact requirements were derived from D3.15: Detailed design of the EPSP plug (Svoboda, et. al., 2015). The inner plug was constructed using glass fibre low pH shotcrete. The concrete was required to fulfil the following requirements:

- pH value of the leached water below 11.7 (in less than 60 days according to R-12-02)
- hydraulic conductivity of  $K < 10^{-8}$ m/s
- uniaxial strength (cylindrical) of a minimum of 30MPa, recommended 40MPa
- flexural strength (first peak – at crack creation) of a minimum of 3MPa, recommended 5MPa
- crack size  $< 0.2$ mm; no pass through the cracks
- recommend micro silica/cement ratio: 50/50
- minimum amount of fibres of  $3\text{kg/m}^3$

Although the requirements on outer plug were less strict (technology not prescribed, pH, fibres) it was made from shotcrete following the same procedure as that used for the inner plug; the use of fibres was not a compulsory requirement. In addition, the same concrete composition was used (as recommended).

### 3 THE LABORATORY TESTING PLAN

Details of the laboratory testing plan and the relevant responsible persons are provided in the following table (Tab. 1) as defined by DOPAS Deliverable 3.16 - Testing plan for the EPSP laboratory experiment (Vašíček et. al., 2013). Interim laboratory results have already been provided in D3.17 (Vašíček et. al., 2014).

Number of series of initial tests on the bentonite, (shot)concrete mixture, rock samples and grouting substances were commencement in 2013 and most of the tests were completed in mid-2015.

The testing procedures conducted by the winner of the “EPSP construction – phase 1” public tender (W1 in the table – Arcadis a. s.) were delayed due to administrative delays (more details on work schedule in D3.20: EPSP plug test installation report, Svoboda (2016). This delay led to a further delay with concern to the subsequent “EPSP construction – phase 2” tender and related construction work including a series of verification tests conducted by the successful bidder (W2 in the table - Metrostav a. s.).

During negotiations on the “EPSP construction – phase 2” contract a number of tests concerning concrete were added to the programme in accordance with a mutual agreement between the CTU and Metrostav a. s. aimed at providing for improved inspection access with concern to both fresh and hardened concrete (immediately following application and after 28 days). Two types of initial tests (moduli) were removed from the testing plan since it was decided that they played no crucial role in terms of quality control. All the changes are noted in Tab. 1 which presents the final status with regard to laboratory testing.

Responsibility for the various tests was distributed among the three Czech DOPAS participants – the CTU in Prague, SÚRAO and ÚJV Řež, a. s. Verification tests were conducted principally by subcontractors appointed by SÚRAO (the “EPSP construction – phase 1” tender on gallery improvements, drilling and grouting) and the CTU (the “EPSP construction – phase 2” tender on EPSP construction).

Tab. 1- Testing plan and final status of the tests

Type of test	Material	Parameter	Responsible institution (person)	Test procedure/ Standard	Test and material conditions (size of samples, density, water content...)	Final status	Details
input	Bentonite	Hydraulic conductivity	CEG CTU (Vašíček)	ČSN CEN ISO/TS 17892-11 Geotechnical investigation and testing - Laboratory testing of soil - Part 11: Determination of permeability by constant and falling head methods	compacted powder, dry densities 1100-1800kg/m <sup>3</sup>	done	
input	Bentonite	Swelling pressure	CEG CTU (Vašíček)	Testing without volume change, internal description following Dixon et. al., 1999; procedure available on Projectplace	compacted powder, dry densities 1100-1800kg/m <sup>3</sup>	done	
input	Bentonite	Hydraulic conductivity	CEG CTU (Vašíček)	ČSN CEN ISO/TS 17892-11 Geotechnical investigation and testing - Laboratory testing of soil - Part 11: Determination of permeability by constant and falling head methods	pellets compacted to dry densities 1100-1800kg/m <sup>3</sup>	done	dry density range was changed to reflect the more realistic values of the bentonite part of the EPSP (1000 – 1500kg/m <sup>3</sup> )
input	Bentonite	Swelling pressure	CEG CTU (Vašíček)	Testing without volume change, internal description following Dixon et. al., 1999; procedure available on Projectplace	pellets compacted to dry densities 1100-1800kg/m <sup>3</sup>	done	
input	Bentonite	Thermal conductivity, heat capacity	CEG CTU (Vašíček)	ISOMET 2114 device, manual	powder - compacted, dry densities 1100-1800kg/m <sup>3</sup>	done	
input	Bentonite	Specific density	CEG CTU (Vašíček)	ČSN CEN ISO/TS 17892-3 - Geotechnical investigation and testing - Laboratory testing of soil - Part 3: Determination of particle density - Pycnometer method	powder	done	
input	Bentonite	Atterberg limits	CEG CTU (Vašíček)	ČSN CEN ISO/TS 17892-12: Geotechnical investigation and testing - Laboratory testing of soil - Part 12: Determination of Atterberg limits	powder	done	
input	Bentonite	Hydraulic conductivity	UJV (Večerník, Gondolli)	ČSN CEN ISO/TS 17892-11 Geotechnical investigation and testing - Laboratory testing of soil	dry densities 1100-1800kg/m <sup>3</sup>	done	

Type of test	Material	Parameter	Responsible institution (person)	Test procedure/ Standard	Test and material conditions (size of samples, density, water content...)	Final status	Details
input	Bentonite	Gas permeability	UJV (Večerník, Gondolli)	internal procedure based on ČSN CEN ISO/TS 17892-11 Geotechnical investigation and testing - Laboratory testing of soil	dry densities 1100-1800kg/m <sup>3</sup>	removed from the testing plan	
input	Bentonite	Porosity	UJV (Večerník, Gondolli)	internal procedure	dry densities 1100-1800kg/m <sup>3</sup>	done	
input	Bentonite	Swelling pressure	UJV (Večerník, Gondolli)	internal procedure based on ČSN CEN ISO/TS 17892-11 Geotechnical investigation and testing - Laboratory testing of soil	dry densities 1100-1800kg/m <sup>3</sup>	done	
technology	Bentonite	Manufacturing and mixture selection	CEG CTU (Šťáštka)	Selection of Czech pellet producer with suitable manufacturing technology	mixtures of various pellet types/ particle fractions	done	selected fraction was used for the bentonite sealing plug of the EPSP
technology	Bentonite	Spraying and compaction field tests	CEG CTU (Šťáštka)	Internal procedure	mixtures of various particle fractions/ pellet types	done	selected technology setting was used during bentonite sealing plug installation
input	Concrete	Thermal conductivity, heat capacity	CEG CTU (Vašíček)	ISOMET 2114 device, manual	samples taken during installation according to the Standard	done	
Verification (moved from input set)	Concrete	Compressive strength	W2 (CTU, Vašíček)	ČSN EN 12390-3 (731302) - Testing of hardened concrete	samples taken during installation, according to the Standard	Done (on both concrete plugs)	Certain tests on the concrete (both fresh and hardened) were added to the testing plan in the form of verification tests during and after installation (not included in D3.16) as more important for quality control purposes (during application and after 28 days). Thus two of the initial tests were removed from the initial testing plan.
input	Concrete	Static modulus of elasticity	W2 (CTU, Vašíček)	ČSN ISO 6784 (731319) - Concrete. Determination of the static modulus of elasticity in compression	samples taken during installation, according to the Standard	removed from the testing plan	
input	Concrete	Static modulus of deformation	W2 (CTU, Vašíček)	ČSN ISO 6784 (731319) - Concrete. Determination of the static modulus of elasticity in compression	samples taken during installation, according to the Standard	removed from the testing plan	

Type of test	Material	Parameter	Responsible institution (person)	Test procedure/ Standard	Test and material conditions (size of samples, density, water content...)	Final status	Details
input	Concrete	Composition and pH of leachates	UJV (Večerník)	based on SKB report R-12-02 (Alonso et. al., 2012)	leaching into distilled water	done	
input	Concrete	Hydraulic conductivity	UJV (Večerník)	based on ČSN CEN ISO/TS 17892-11	cylindrical sample	done	Conducted by external laboratory
input	Concrete	Porosity	UJV (Večerník)	mercury porosimetry/ water immersion method	external analysis / cubes, discs	done	Conducted by external laboratory
Verification (moved from input set)	Concrete	Compressive strength, Depth of penetration of water	W2 (UJV, Večerník)	ČSN EN 12390-3 (731302) - Testing of hardened concrete	Compressive strength, Depth of penetration of water under pressure	Strength test done by W2, penetration test removed	moved from input to verification tests
input	Grouting substances	Interactions	UJV (Večerník)	Internal procedure for interaction processes	grouting/plug materials/plug environment	done	
input	Rock samples	Compressive strength	W1 (SURAO, Dvořáková)	ČSN EN 1926 - Natural stone test methods - Determination of uniaxial compressive strength	drilled cores	done	see in Záruba, 2015
input	Rock samples	Static modulus of deformation	W1 (SURAO, Dvořáková)	ČSN ISO 6784 (731319) - Concrete. Determination of static modulus of elasticity in compression	drilled cores	done	
input	Rock samples	Density	W1 (SURAO, Dvořáková)	e.g. ČSN EN ISO 17892-2	drilled cores	done	
input	Rock samples	Hydraulic conductivity	UJV (Večerník)	Changes in rock permeability due to grouting	drilled cores	done	Conducted by external laboratory
input	Rock samples	Porosity	UJV (Večerník)	Mercury porosimetry / water immersion method	external analysis/ cubes, discs of plug material	done	Conducted by external laboratory
input	Rock massif	Modulus of deformation	W1 (SURAO, Dvořáková)	Loading plate	field test (testing niche)	done	Sosna et. al., 2014a

Type of test	Material	Parameter	Responsible institution (person)	Test procedure/ Standard	Test and material conditions (size of samples, density, water content...)	Final status	Details
input	Rock massif	Modulus of deformation	W1 (SURA, Dvořáková)	Menard pressiometer test, Eurocode 7- Part 2	field test, 2 boreholes (5m long)	done	Sosna et. al., 2014a
input	Rock massif	Hydraulic conductivity	W1 (SURA, Dvořáková)	Hydraulic pressure test	field test, 5 boreholes (5m)	done	Sosna et. al., 2014b
verification	Bentonite	Hydraulic conductivity	CEG CTU (Vašíček)	ČSN CEN ISO/TS 17892-11 Geotechnical investigation and testing - Laboratory testing of soil - Part 11: Determination of permeability by constant and falling head methods	pellets compacted to dry densities 1100-1800kg/m <sup>3</sup>	done	
verification	Bentonite	Hydraulic conductivity	UJV (Večerník, Gondolli)	Based on ČSN CEN ISO /TS 17892-11	plug material	done	
verification	Concrete	Hydraulic conductivity	UJV (Večerník)	Internal procedure	plug material	done	
verification	Concrete	Porosity	UJV (Večerník)	mercury porosimetry / water immersion method	external analysis / cubes, discs of plug material	done	Conducted by external laboratory
verification	Concrete	Composition and pH of leachate	UJV (Večerník)	based on SKB report R-12-02 (Alonso et. al., 2012)	leaching into distilled water	done	
verification, added	Concrete	Flexural strengths (first peak, ultimate and residual)	W2 (CTU, Vašíček)	ČSN EN 14488-3 Testing of sprayed concrete. Flexural strengths (first peak, ultimate and residual) of fibre-reinforced beam specimens	samples taken during installation, according to the Standard	done (on both concrete plugs)	added to the testing plan before installation, not in D3.16
verification, (moved from input set)	Concrete	Hydraulic conductivity	W2 (CTU, Vašíček)	based on ČSN CEN ISO/TS 17892-11	samples taken during installation, according to the Standard	done (on the inner concrete plug)	added to the testing plan before installation, not in D3.16

Type of test	Material	Parameter	Responsible institution (person)	Test procedure/ Standard	Test and material conditions (size of samples, density, water content...)	Final status	Details
verification, added	Concrete	Density (hardened concrete)	W2 (CTU, Vašíček)	ČSN EN 12390-7 Testing hardened concrete. Density of hardened concrete.	samples taken during installation, according to the Standard	done (on both concrete plugs)	added to the testing plan before installation, not in D3.16
verification, added	Concrete	Consistency (fresh concrete)	W2 (CTU, Vašíček)	ČSN EN 12350-5 Testing fresh concrete. Flow table test.	samples taken during installation, according to the Standard	done (on both concrete plugs)	added to the testing plan before installation, not in D3.16
verification, added	Concrete	pH	W2 (CTU, Vašíček)	Based on SKB report R-12-02 (Alonso et. al., 2012)	samples taken during installation, according to the Standard	done (on both concrete plugs)	added to the testing plan before installation
verification	Grouting substances	Interactions	ÚJV (Večerník)	Internal procedure	grouting/plug materials/plug environment	done	
physical model	Bentonite, concrete, granite	Long-term stability	ÚJV (Večerník, Gondolli)	Internal procedure	Cylindrical sample: bentonite, concrete, granite	done	
physical model	Bentonite, concrete	Water content in sample	ÚJV (Trpková, Večerník, Gondolli)	Internal procedure	App. 50cm long cylindrical sample, gradual saturation, material interaction studies	done	

*note: W1 - winner 1 - Arcadis a. s. - winner of the public tender (no. 1, by SURAO) on grouting and drilling work  
W2 - winner 2 - Metrostav a. s. - winner of the public tender (no. 2, by CTU) on plug construction*

## 4 RESULTS OF LABORATORY TESTS

The following chapters present the final results obtained from laboratory testing. The work performed is presented in the form of chapters according to the institution responsible for delivery.

A bentonite material accorded the code number B75\_2013 was selected for the construction of the DOPAS EPSP seal. B75 bentonite consists of a Czech Ca-Mg industrially milled and sifted non-activated bentonite; it was supplied in 2013. Laboratory tests were performed on the material in order to verify its properties. In some cases the results of B75\_2010 testing were used for comparison purposes (B75\_2010, i.e. B75 material supplied in 2010, examined in 2010-2013, e.g. Červinka & Hanuláková, 2013 and Červinka et. al., 2012).

The type of water (distilled and/ or “SGW - synthetic granitic water”; for details of the composition see Tab. 2) used during laboratory testing is indicated in each sub-chapter. Distilled water was used when required by the standard (testing method) or when results comparable to previous results were required. The determination of the composition of laboratory prepared SGW (Havlová et al., 2010) was based on a statistical evaluation of the composition of the groundwater of Czech granite massifs at depths of between 20 and 200 meters. In some cases, tests were conducted using “Josef” (facility) groundwater (collected in the vicinity of the EPSP experimental drift).

Tab. 2 - Composition of SGW – Synthetic granitic water (mg/l)

Na	K	Ca	Mg	Cl	SO <sub>4</sub>	NO <sub>3</sub>	HCO <sub>3</sub>	F
10.6	1.8	27.0	6.4	42.4	27.7	6.3	30.4	0.2

### 4.1 Work performed by the Centre of Experimental Geotechnics (CEG), CTU in Prague

#### 4.1.1 Time schedule of the tests

The basic laboratory tests were aimed at the estimation of the specific density and Atterberg limits of the bentonite powder. This was followed by the determination of hydraulic conductivity and swelling pressure with regard to compacted samples (several dry density values). Distilled water was used in all the tests. The tests were concluded in early 2014.

The testing of the most appropriate technology for the manufacture of the pellets, in cooperation with potential Czech producers, was carried out from May to November 2013. Tests aimed at determining the most suitable mixture for spray technology purposes were conducted up to mid-2014. Verification of the technology to be employed for pellet emplacement purposes (a combination of plate compaction and spraying) and tests supporting the selection of the most suitable spraying machinery and mixture (with or without ice) were also performed in 2014.

Subsequently, large test cells to be used for the estimation of the hydraulic conductivity and swelling pressure of the pellet samples were constructed and employed for the verification of the behaviour of the pellets; distilled water was used as the liquid medium. The first phase of testing focused on the verification of the functioning of the new cells (by means of a comparison of the test results from samples with the same parameters in both normal sized and large cells) which was followed by the testing of the pellets proper. These long-term tests continued until mid-2015.

The CTU’s responsibilities also included the inspection of the results of verification tests conducted by Metrostav a. s. (the winner of the “EPSP construction – phase 2” tender on EPSP construction) on concretes prior to and following plug construction in late 2014 and mid-2015.

During the EPSP construction phase the CTU was responsible for the emplacement of the bentonite seal (mid-2015). In-situ sampling was conducted so as to monitor the achieved dry density of both the pellet and sprayed layers; the various requirements were fulfilled with regard to the whole volume of the seal. More extensive details are provided in D3.20: the EPSP plug test installation report (Svoboda et. al., 2016).

#### 4.1.2 Results of input laboratory tests on the bentonite

- The average of the measured values of specific density was  $2.855\text{g/cm}^3$ .
- The average liquid limit value was found to be 171% using distilled water for testing purposes. This value falls within the anticipated liquid limit range.
- The swelling pressure of bentonite B75\_2013 is in the range of approximately 1 to 8MPa for a dry density value of  $1.26\text{--}1.64\text{g/cm}^3$ . The dependence of swelling pressure on dry density is shown in Figure 2.
- The swelling pressure value for a dry density value of  $1.4\text{g/cm}^3$  was determined at 2MPa which indicates that **swelling pressure behaviour corresponds to the initial assumption** (see Chapter 2; taken from DOPAS Deliverable D2.1, White et. al., 2013).
- The hydraulic conductivity of bentonite B75\_2013 is in the range  $10^{-12}$  -  $10^{-13}\text{m/s}$  for a dry density value of  $1.26\text{--}1.64\text{g/cm}^3$ ; dependence on dry density is shown in Figure 3.
- **The hydraulic conductivity value determined corresponds to the initial assumption** (see Chapter 2; taken from DOPAS Deliverable D2.1, White et. al., 2013).

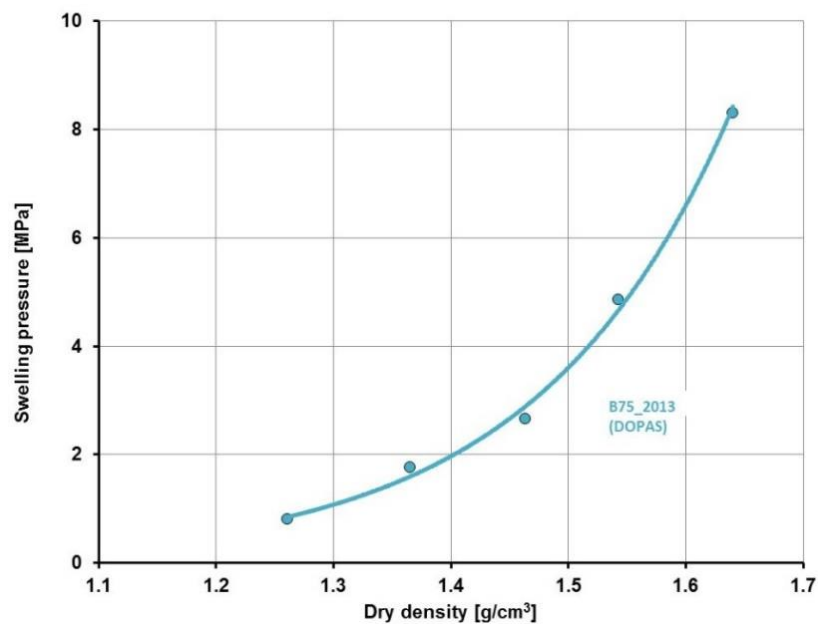


Figure 2 – Swelling pressure of bentonite B75\_2013

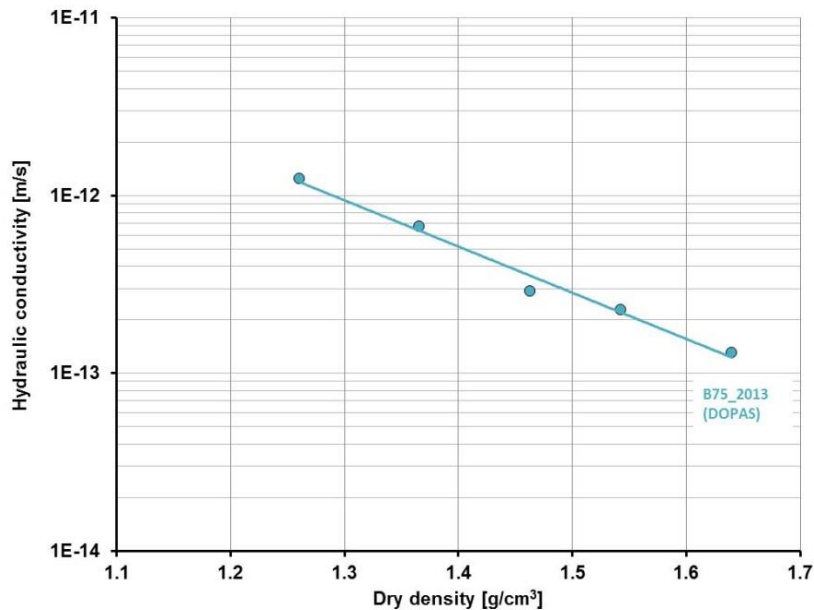


Figure 3 - Hydraulic conductivity of bentonite B75\_2013

#### 4.1.3 Thermo-physical properties

The determination of thermal conductivity and heat capacity was conducted by the CEG by means of the ISOMET 2114 device (Applied Precision, 2015) on powder and compacted samples at two water content levels (6% and 20%).

The ISOMET 2114 consists of a portable hand-held measuring instrument designed for the direct measurement of the heat transfer properties of a wide range of isotropic materials including cellular insulating materials, plastics, glass and minerals. It is equipped with two optional types of measurement probe – needle probes for soft materials and surface probes for hard materials and applies a dynamic measurement method. The surface probes are intended for the taking of measurements on solid and/or hard materials. A flat surface of at least 60mm diameter suffices for the use of the probe. The requirement for surface flatness accuracy increases with the increasing thermal conductivity value of the tested material. The required minimum thickness of the material to be evaluated ranges from 20mm to 40mm depending on its conductivity. (Applied Precision, 2014).

Homogenous samples of B75 (w = 6% and 20%) with various dry densities were tested. In addition, pellets (B75\_PEL 12, w = 16%) at densities close to those expected in the sealing section of the EPSP were subjected to examination. Thermal conductivity is shown in Figure 4 and volume heat capacity in Figure 5.

Thermo-physical properties are important in cases where heat transfer can be expected. Whereas this property is not directly relevant to the EPSP experiment, it will be necessary to determine such parameters in connection with the construction of the deep geological repository. Moreover, heat is generated during the hydration of concrete. Therefore, tests were performed in order to provide the material parameters which will allow the potential modelling of EPSP behaviour from the conclusion of the construction phase. No limit values were set either for thermal conductivity or heat capacity.

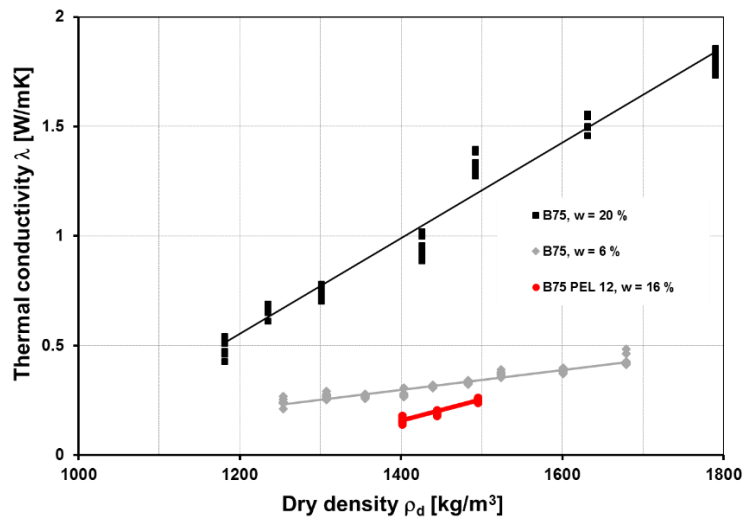


Figure 4 – Thermal conductivity of the homogenous samples ( $w = 6\%$  and  $20\%$ ) and pellets ( $w = 16\%$ )

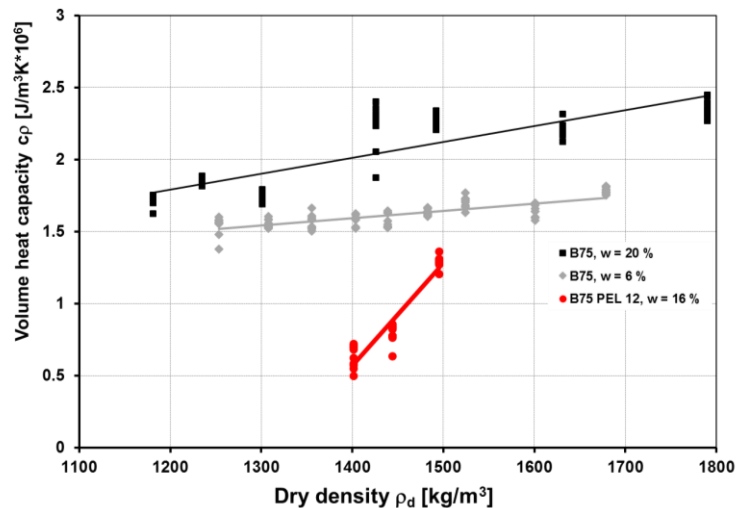


Figure 5 – Volume heat capacity of the homogenous samples ( $w = 6\%$  and  $20\%$ ) and pellets ( $w = 16\%$ )

#### 4.1.4 Comparison of B75\_2013 with other Czech bentonites

This chapter provides a comparison of the geotechnical parameters of bentonite B75\_2013 with a selection of other Ca-Mg bentonites available in the Czech Republic. Activated bentonite SAB65 (Sabenil 65, produced by Keramost, Plc.), which is characterized by significantly higher liquid limit and swelling pressure and lower hydraulic conductivity values, was also subjected to comparison.

It was verified that bentonite B75\_2013 attains values of hydraulic conductivity and swelling pressure typical for Ca-Mg Czech swelling clays (Figure 6 and Figure 7).

The liquid limit value of B75\_2013 lies between that of Ca-Mg bentonite from the Černý Vrch locality and gently activated B75\_2010 (Figure 8; more on B75\_2010 is available in Červinka & Hanuláková, 2013 and Červinka et. al., 2012).

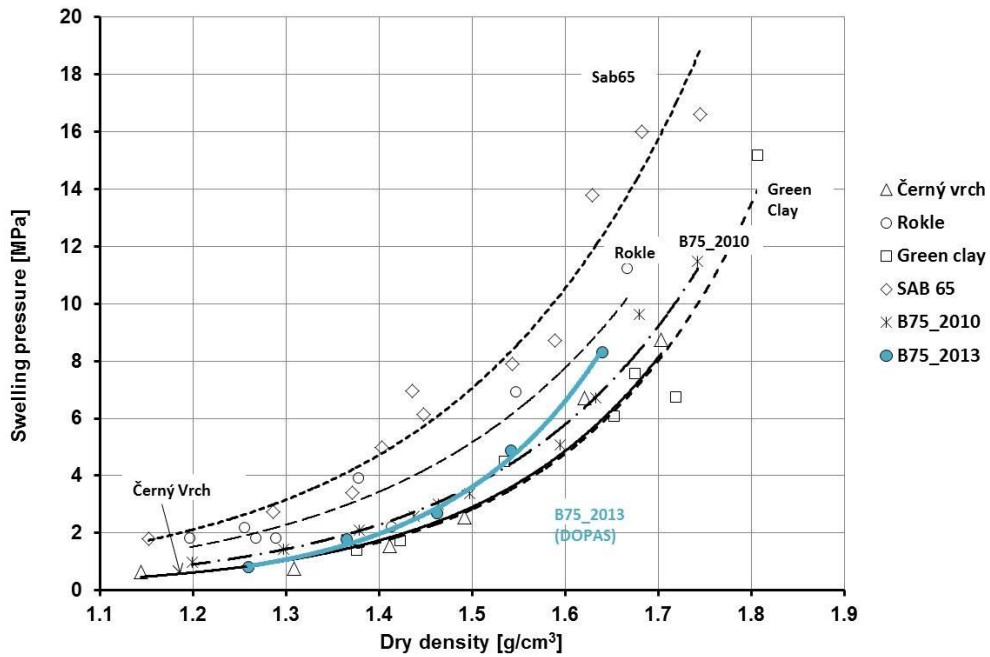


Figure 6 – Comparison of the swelling pressure of B75\_2013 and other Czech bentonites

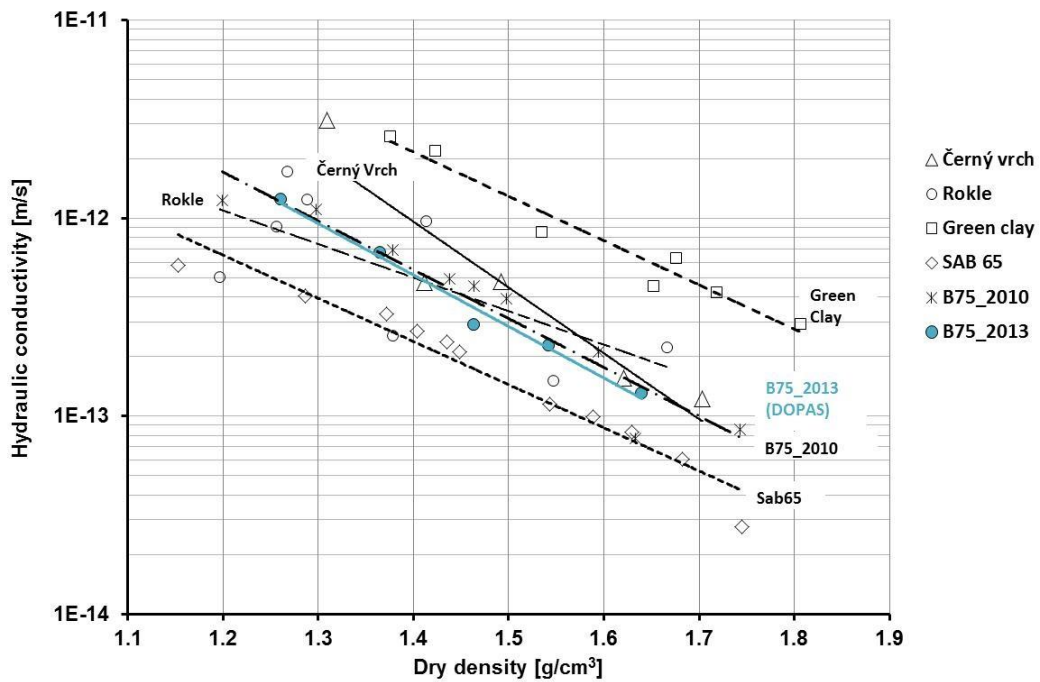


Figure 7 – Comparison of the hydraulic conductivity of B75\_2013 and other Czech bentonites

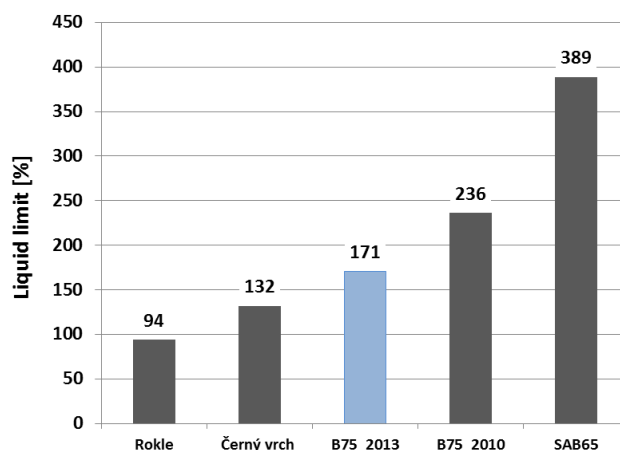


Figure 8 – Comparison of the liquid limit of B75\_2013 and other Czech bentonites

#### 4.1.5 Pellet manufacturing technology, quality verification and emplacement technology

The bentonite pellet zone comprises B75 bentonite, a natural and high-smectite-content Ca-Mg bentonite. The purpose of the bentonite is to seal and absorb/adsorb any water that leaks across the inner concrete plug. The bentonite zone is 2m long.

##### 4.1.5.1 Pellet production

The aim of this part of the project was to find Czech producers of bentonite pellets of a sufficiently high quality level and the production capacity needed for EPSP purposes. It involved establishing contacts with various potential industrial partners in order to verify the quality of their products, i.e. the detailed testing of the relevant properties in terms of use in the EPSP seal. The key issue concerned attaining the ideal dry density level following pellet emplacement, the verification of which involves the use of a range of techniques: free fall pouring, vibration, spraying and plate compaction.

B75 is produced in powder form which is not ideal for sealing plug purposes due to the low level of compaction. Therefore, the first stage involved the selection of the best compaction technology commercially available in the Czech Republic. Eventually, three technological processes were selected for further consideration.

The first method originated from a factory which produces compacted kaolin clay pellets (cylinders with a diameter of 12mm) by means of a roller compaction machine. A number of tests were conducted concerning the manufacture of the bentonite pellets, the main aim of which was to determine the conditions for the industrial compaction and production of the bentonite pellets with the most suitable dry density value. The final dry density of the compacted pellets depends on the water content of the material; B75\_2013 bentonite had to be moistened prior to compaction. The relationship of dry density and various water content levels is shown in Figure 9 (Štástka, 2013). Subsequently, material with a water content of around 16% was selected for further experimental testing. The pellets selected from this producer, code-named B75 PEL\_12, have a diameter of 12mm, a length of up to 4cm (Figure 10) and a dry density value of 1.80-1.85g/cm<sup>3</sup>.

The second compaction method was based on a small roller compaction machine which produced bentonite pellets with a diameter of 8mm. This method, however, was not selected for further testing due to the low level of bentonite compaction and the amount of time required for production.

The third method considered (employing a roller mill) was the result of consultation with a Czech bentonite production company which was followed by laboratory testing. The pellets (fragments of highly-compacted bentonite plate) produced employing this procedure are not available commercially but the machinery involved is in common use. Laboratory testing revealed a good level of compaction (dry density 1.70-1.98g.cm<sup>-3</sup>) with a relatively low water content value. The advantage of this

technology is the production of pellet fragments with various sizes. It allows mixing in various proportions in order to achieve the best dry density value following emplacement. The resulting material was codenamed B75\_REC (Figure 11). A comparison of the dry density and water content of selected B75\_PEL\_12 and B75\_REC pellets is provided in Figure 12.

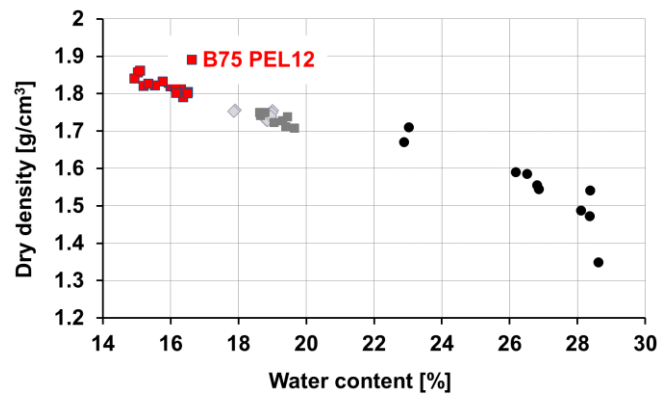


Figure 9 – Range of water content and dry density values of compacted bentonite produced by the roller machine – the red dots show B75\_PEL\_12 selected for further development



Figure 10 – Compacted bentonite pellets B75\_PEL\_12 from the roller compaction machine (Štástka, 2013)



Figure 11 – Compacted bentonite B75\_REC

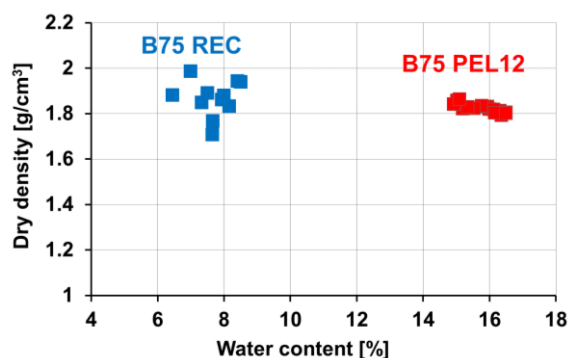


Figure 12 – Comparison of the dry density and water content values of selected materials B75\_PEL\_12 (red dots) and B75\_REC (black dots).

#### 4.1.5.2 Hydraulic conductivity and the swelling pressure of the pellets

New large cells for the testing of the hydraulic conductivity and swelling pressure of pellet-form bentonite were designed for DOPAS laboratory testing purposes. The cylindrical samples were significantly larger (12cm in diameter and 5cm high, Figure 13) than the reference samples for the testing of compacted bentonite powder (3cm in diameter and 2cm high).

Initially, it was necessary to test the new cells so as to ensure that there were no errors or differences with regard to the procedure employed in connection with the reference samples. Powder-form samples were tested in new cells and the results obtained were compared to the reference results; no differences were discovered either in terms of hydraulic conductivity (Figure 15) or swelling pressure (Figure 14).



Figure 13 – A large cell and a pellet-form bentonite sample prior to and following testing

Following the conclusion of the initial testing phase, a pellet-form material (B75\_PEL12) was tested. Freely poured pellets were dynamically compacted so as to achieve a dry density level of around  $1.4 \text{ Mg/m}^3$  (the dry density parameter required with regard to the sealing section of the EPSP experiment). The swelling pressure of the pellet-form material was found to be similar to that of the powder-form samples (see Figure 14); however, the hydraulic conductivity of the pellet-form material was lower (in the range of  $10^{-12}$ - $10^{-13}$  m/s). It was assumed that the decrease in hydraulic conductivity was most probably the result of the testing procedure which can lead to the clogging of the sample in its upper part with smaller particles when 1MPa of saturation pressure is applied from the bottom part at the beginning of the saturation phase (water flow within the cell is from the bottom upwards). Expert literature reports no differences in hydraulic conductivity and swelling pressure between powder-form and pellet-form materials (Karnland et al. 2007 and Hoffmann et al. 2007).

The surrounding rock in the EPSP experimental niche was sealed by means of grouting to a distance of 5m of the original excavation and the resulting hydraulic conductivity level was tested ( $<10^{-10}$  m/s) (D3.20, Svoboda et. al., 2016). All the values for the compacted bentonite (pellets) are at least two orders of magnitude lower and therefore pellets exhibits better - less permeable – sealing ability than surrounding grouted rock.

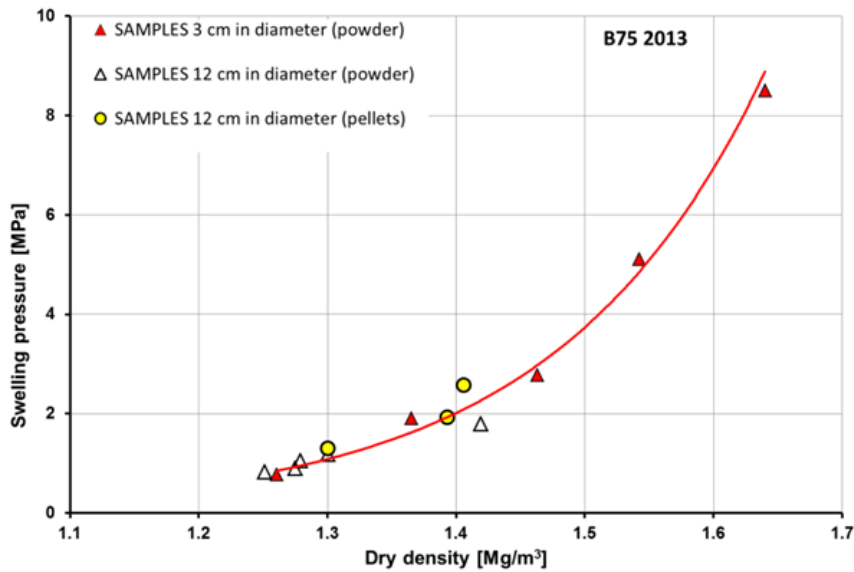


Figure 14 – Swelling pressure of B75 material related to dry density. The red triangles with the red line represent the reference samples (3cm in diameter) compacted from powder, the white triangles represent large samples (12cm in diameter) compacted from powder and the yellow circles show the results from large samples prepared from pellets.

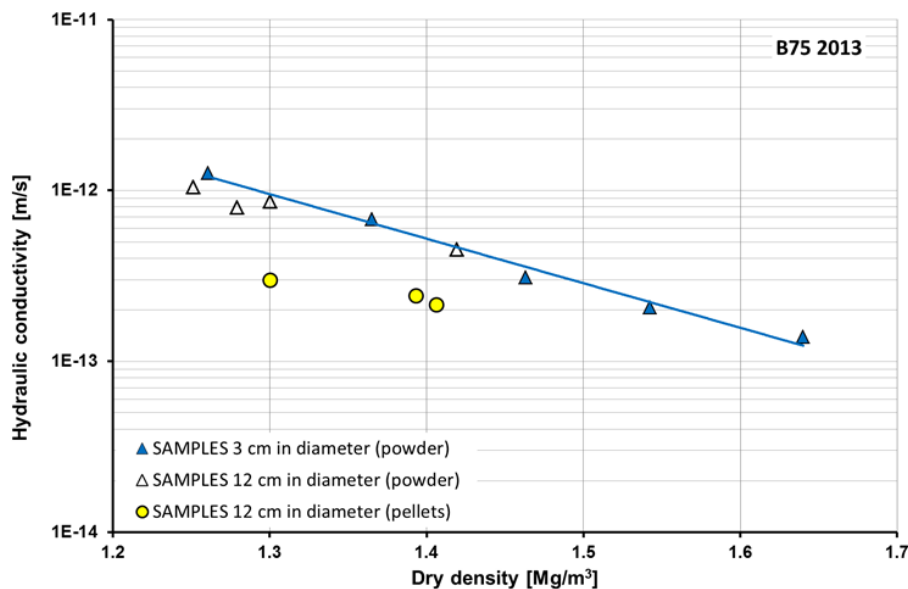


Figure 15 – Hydraulic conductivity of B75 material related to dry density. The blue triangles (and blue trend line) represent the reference samples (3cm in diameter) compacted from powder, the white triangles represent the large-scale compacted powder samples (12cm in diameter) and the yellow circles show the results of pellet-form large samples.

#### 4.1.5.3 Selection of the pellet mixture

Tests were conducted on mixtures based principally on B75\_REC 0.8-5 (grains 0.8-5) aimed at the verification of dry density following pellet emplacement. One of the samples was mixed according to the Fuller grain size distribution (without fine particles below 0.5mm; maximum grain diameter 15mm) and code-named B75\_REC\_F. The particle size distribution of the pellets is shown in Figure 16.

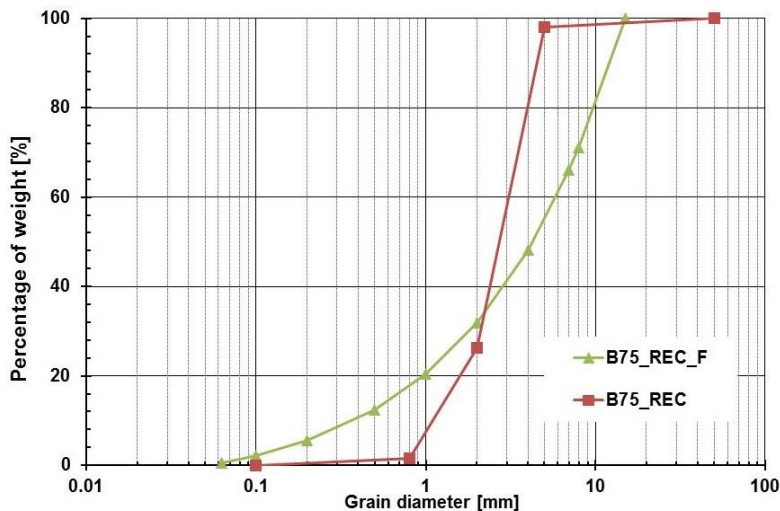


Figure 16 – Particle size distribution of pellets made from B75\_2013

Five methods were tested for the emplacement of the selected materials (B75\_REC 0.8-5; B75\_REC\_F; B75\_PEL\_12): the free fall pouring, free fall pouring with vibration, spraying using a concrete spray machine, spraying (with ice) using Mixokret machine and plate compaction methods. The first results revealed the impact of vibration on the dry density of the tested materials (Tab. 3). Results gained by using other methods (spraying, plate compaction) are presented in following subchapters, as results of the medium scale tests.

Tab. 3 - Dry density results [g/cm<sup>3</sup>] following initial compaction tests

Material/ Emplacement	Free fall pouring	Pouring with vibration
B75_REC 0.8-5	1.11	1.20
B75_REC_F	1.39	1.55
B75_PEL_12	0.98	1.12

It is clear from Tab. 3 that B75\_REC F approximates very well with the required limit for emplaced dry density - 1.4g.cm<sup>-3</sup> - using the free pouring method only. Vibration during emplacement increases the value of dry density to 1.55g.cm<sup>-3</sup>. It was expected that spraying and/or plate compaction would also increase the value of dry density in the case of both the free fall pouring and/or vibration methods.

The results were considered particularly satisfactory, i.e. it was considered that the use of the B75\_REC F mixture for EPSP purposes would ensure a sufficient level of dry density within the bentonite seal. However, preference was subsequently accorded to B75\_REC 0.8-5 and B75 PEL 12 for the “medium scale tests” which followed since the mixing of several tons of mixture according to Fuller’s curve would simply not be feasible.

#### 4.1.5.4 Pellet emplacement tests at the “medium” scale

It was planned that a bentonite-ice mixture would be used for the DOPAS sealing section. Therefore, several tests were performed in order to verify the feasibility of its use with respect to the technology available and the specific requirements of the EPSP experiment (the total amount of material required, capacity per hour, distance from the ice source etc.). Compaction employing ordinary plates and spraying technology was also tested at the larger scale so as to verify the quality and homogeneity of the compacted layer; B75\_REC 0.8-5 and B75 PEL 12 were used for testing purposes.

#### 4.1.5.4.1 Emplacement of the pellet-ice mixture employing the Mixokret machine

The mixture of pellets and ice had previously been tested in the context of other projects conducted at the CEG. The results led to the determination of the required compaction level of the EPSP samples. The spraying technology was tested by means of the Mixokret machine. A modified process was designed for the purpose of medium-scale testing involving the loading of the machine with an enhanced amount of the mixture (B75\_REC 0.8-5), and a steel box (0.4m x 0.4m x 0.4m = 0.064m<sup>3</sup>) was constructed into which the material was sprayed. Subsequently samples were removed from the box for the evaluation of the dry density and water content following spraying. One disadvantage of the use of the Mixokret machine is that it is not a continual process. The first step in the testing process consisted of the preparation of the Mixokret machine and an air compressor, which was followed by the filling of the machine with bentonite pellets. The machine was then switched on and crushed ice added. Spraying commenced following the completion of the mixing process. Each spraying cycle consisted of approximately 10 individual shots from the machine delivering a total amount of the mixture of 0.01m<sup>3</sup>. Once the machine was empty it was refilled with the mixture and the next spraying cycle commenced. Two medium-scale tests were prepared for EPSP purposes the main aims of which were to discover the capabilities of the spraying of the pellet and crushed ice mixture (mixture 4:1) and the verification of the dry density of the material following spraying. The material was sprayed at a rate of 0.064m<sup>3</sup> every 2 hours. The testing of the dry density of the samples revealed a compaction value of in excess of 1.42g/cm<sup>3</sup> with a water content of 25%; however, the total compaction level in the box was less due to the material in the corners of the box being compacted to a lesser degree. The average dry density therefore (calculated from the volume of the box and the weight of the material inside the box) was determined at 1.3g/cm<sup>3</sup> for medium-scale tests.



Figure 17 – The Mixokret machine for the spraying of bentonite pellets with crushed ice and the filling of the steel box for the medium-scale tests

#### 4.1.5.4.2 Emplacement of pellets employing compaction plates

Both the B75 PEL 12 and B75 REC 0.8-5 materials were compacted into a testing box with a volume of 0.25m<sup>3</sup> using various compaction machines. Because of its higher water content B75 PEL 12 proved to be more suitable for the compaction process because of the dust level and dry density following compaction (see Tab. 4). The application capacity was 0.25m<sup>3</sup> per 30 minutes for both pellet materials.

Tab. 4 - Dry density results [Mg/m<sup>3</sup>] following tests with compaction plates

Pellets	Compaction machine [weight, compaction force]	Average density [Mg/m <sup>3</sup> ]	Average dry density [Mg/m <sup>3</sup> ]
B75_REC_0.8-5	NTC compaction plate: 105kg, 20kN	1.43	1.33
B75_PEL_12	NTC compaction plate: 105kg, 20kN	1.67	1.44
B75_PEL_12	Ammann compaction plate: 500kg, 65kN	1.75	1.49
B75_PEL_12	Masalta vibrating tamper: 75kg, 14kN	1.71	1.46



Figure 18 – Compaction plate tests

#### 4.1.5.4.3 Emplacement of the pellet mixture using sprayed clay technology

The B75 REC 0.8-5 material was used for spraying test purposes and results subsequently proved that the required dry density limit is achievable ( $1.42\text{Mg/m}^3$  with a water content of 25%). This method has potentially a number of drawbacks including a high rebound ratio (up to 60%) and high dust levels. Optimal procedure must be strictly followed to minimize these consequences.



Figure 19 – Spraying machine SSB14 and a nozzle

#### 4.1.5.4.4 Conclusions from the emplacement tests

Various compacting technologies and machines providing desirable results (sufficient dry density) were tested. An overview of the dry density values attained is provided in Tab. 5.

Tab. 5 - Dry density results [ $\text{g/cm}^3$ ] from all the emplacement techniques (bold – selected for EPSP)

Material/ Technology	Free fall pouring	Pouring with vibration	<b>Spraying (SSB machine)</b>	Spraying with ice (Mixokret)	<b>Compaction plate (NTC/ Masalta)</b>
<b>B75_REC 0.8-5</b>	1.11	1.20	<b>1.42 (w=25%)</b>	1.32 (w=25%)	1.33
B75_REC_F	1.39	1.55	Not tested	Not tested	Not tested
<b>B75_PEL_12</b>	0.98	1.12	Not tested	Not tested	<b>1.44/ 1.46</b>

The above parameters are comparable to the results obtained at other institutions. Tab. 6 shows experience obtained in the emplacement of bentonite pellets by, particularly, SKB and Posiva (Dixon et. al., 2011).

The achieved dry density was not only the criteria for final selection of technologies to be used in EPSP. Ability to install/ compact sufficient amount of material per time unit (throughput) was another key parameter.

Due to time constraints with regard to bentonite emplacement, it was decided that the clay and ice mixture would not be used; the application machinery for this method has a very limited throughput. Two technologies were selected for the compaction of the pellets used in the EPSP experiment. The main part of the sealing element of the EPSP was constructed by means of the use of ordinary compaction plates using B75\_PEL-12 pellets. Sprayed clay technology using B75\_REC\_0.8-5 was selected for the filling of those spaces which cannot be accessed by classic compaction machines (the space under the roof of the EPSP sealing section).

Tab. 6 - Experience with pellet emplacement (Dixon et. al., 2011)

Table 2-3. Properties and as-placed densities of bentonite pellets, granules and granule-pellet blends examined in deposition tunnel backfill and as tunnel floor materials (openings > 100 mm width).

Material	Pellet Size (mm)	Pellet Production Method	Pellet Dry Density (kg/m <sup>3</sup> )	Installed Dry Density (kg/m <sup>3</sup> )	EMDD (kg/m <sup>3</sup> )	Notes and Compaction Method	Reference
MX-80	13×13×6	Roller	1,910–2,010	1,050–1,135	828–1,015	Backfill and Plug test.	Gunnarsson et. al 2001
MX-80	30×20×12	Roller		920	755	Backfill and Plug Test.	Gunnarsson et. al 2001
MX-80	13×13×6 50:50 mix	Roller and crushed	1,910	1,310	1,120	Dry poured	Gunnarsson et al. 2001
MX-80				1,040	865		De Bock et. al 2008
MX-80		Roller then crushed and screened	2,170 2,320	1,440–1,590	1,250–1,400	Lab tests using < 16 mm Fuller-graded crushed pellets and vibration compaction.	Blümling and Adams 2007
				1,620	1,435	Lab tests using < 20 mm Fuller-graded crushed pellets and vibration compaction.	
				1,090–1,330	910–1,140	Lab tests, not vibrated.	
MX-80	18×18×8	Roller	1,780	932	767	Laboratory determination.	Sandén et. al 2008
Friedland	Granules/ flakes	~8×8×4	1,995–2,075	1,010	573	Laboratory determination.	Sandén et. al 2008
Cebogel QSE	6.5 dia 5–20 long	Extruded cylinders	1,720	943	777	Laboratory determination.	Sandén et. al 2008
Cebogel QSE	6.5 dia 5–20 long	Extruded cylinders	1,810	950–1,080	783–902	Block-rock gap fill in ¼ scale tests.	Dixon et. al. 2008a, b
Cebogel QSE	6.5 dia 5–20 long	Extruded cylinders		990–1,180	819–996	Block-rock gap fill in small-scale tests.	Dixon et. al. 2008a
				473 – 971	371–802	Installed in bench-scale tests.	Riikonen 2009
Milos	< 10	Crushed		1,100	921	Used to fill block-rock gap in backfilling trials.	Dixon et. al 2008a,b
Milos	< 10	Crushed		1,360	1,171	Crushed raw bentonite, tunnel flooring.	Wimelius and Pusch 2008
70% Kunigel 30% Sand	< 5	Crushed blocks	<1,900	1,300	649	Shotclay used in Tunnel Sealing Experiment.	Martino et. al 2008
bentonite-aggregate mix	< 5			950–1,600	500–960	Backfilling mock-ups at URL.	Martino and Dixon 2007
Boom clay		Roller	2,100	1,700	?	50/50 Boom clay pellets and powder Bacchus 2	Voickaert and Bernier 1996
FoCa	25×25×15	Roller	1,890	1,400	?	50/50 pellet/powder mix, Reseal Project Mol Loose pour	Imbert and Villar 2006
			1,890	1,600		Vibrocompacted	
FoCa, Boom Clay		Roller	2,100	1,700	?	Vibratory compaction	Voickaert and Bernier 1996
						Bacchus 2 Project	
Serrala	> 7; 0.4–2	Roller then crushed	2,110–2,130	1,360	1,318	Crushed larger briquettes and 2 size blend, auger installation.	Mayor et. al 2005
Serrala	> 7; 0.4–2	Roller then crushed	2,110	1,450–1,510	1,409–1,469	Crushed larger briquettes and 2 size blend, auger installation.	Nold 2006, Fries 2008
FEBEX		Roller	1,700	1,300–1,400	?	Ca-Mg bentonite installed by conveyor/flinger.	Fuentes-Cantillana and Huertas (2002)
Wyoming	Granule blends	Crushing HCB		1,440–1,510	1,250–1,320	Horizontal tunnel placement trials using crushed HCB blocks as source for granules.	Nold 2006, Fries 2008
Wyoming	Large granules	Crushing HCB		1,390	1,200	Horizontal tunnel placement trials using crushed HCB blocks as source for granules.	Nold 2006, Fries 2008
<b>Tunnel Flooring Material</b>							
Cebogel QSE pellets	6.5 dia 5–20 long	Extrusion		1,150	968	In situ compacted on floor.	Wimelius and Pusch 2008
Mineico granules	< 30 mm and < 10% of < 0.125	Crushed raw bentonite		1,250		In situ compacted on floor; optimal layer thickness ~150 mm.	Wimelius and Pusch 2008

? – mineralogy not defined so EMDD not calculated.

#### 4.1.5.5 Real application of bentonite pellets

The CTU was responsible for the emplacement of the bentonite seal. The EPSP inner plug was cast in November 2014, the bentonite core was emplaced in June 2015 and the outer plug was cast in June 2015. 95% of the sealing section core (bentonite pellets) was vibration-compacted, with the remaining 5% (crown space) emplaced using shot clay technology.

The bentonite was emplaced in horizontal layers with a maximum thickness of 3cm which were subsequently vibration compacted. Electric hammer drills with plates were used for compaction around the measurement sensors, around the drift wall and in the upper part of the drift.

Sprayed clay technology was used for the backfilling of the upper part of the drift. Approximately 5% (1.5m<sup>3</sup>) was backfilled; with B75 REC 0.8-5. The spraying machine selected consisted of the SSB 14 DUO (Filamos Ltd.) machine fitted with an Atlas Copco electric air compressor (working pressure 10 bar, air capacity 350m<sup>3</sup>/h). The application rate was 0.25m<sup>3</sup> per hour with emphasis being placed on following a spraying procedure which best limited the drawbacks inherent in this method.

In-situ sampling was conducted during the construction phase so as to monitor the achieved dry density of the pellet layer. Requirements concerning dry density (1.4Mg/m<sup>3</sup>) were fulfilled throughout the whole volume of the seal. More details are available in D3.20: the EPSP plug test installation report (Svoboda et. al., 2016).



*Figure 20 - Pellet emplacement (compaction)*



*Figure 21 - Upper part of the drift – the space intended for backfilling using spraying technology*



Figure 22 - Shot clay application

#### 4.1.6 Verification tests on concrete during and after installation

The CTU subcontractor, Metrostav a. s. was responsible for verification testing during and after construction. The requirements with concern to tests on the concrete samples were set out in the public tender documentation. Contract negotiations led to the inclusion of a number of additional tests to ensure an improved level of monitoring of both the fresh and hardened concrete (during construction and after 28 days). Two initial tests were removed from the testing plan since it was decided that they were not crucial in terms of quality control.

##### 4.1.6.1 Requirements of the concrete plugs

At the outset of the EPSP experiment, it was decided to use glass-fibre-reinforced low-pH shotcrete for both the inner and outer concrete plugs. The decision was based on previous experience with (steel) fibre shotcrete gathered during the construction of the Hájek gas storage pressure plugs. However, in order to avoid corrosion (and the addition of Fe to the system) glass fibres were selected as the reinforcement material in place of Fe-based materials. These fibres also significantly help in terms of reducing (micro)cracking caused by shrinkage. In addition, lower pH concrete was required in order to limit potential impacts on the bentonite material (more in the D3.20 installation report; Svoboda et. al., 2016).

Exact requirements were derived from D3.15: Detailed design of the EPSP plug (Svoboda, et. al., 2015). The inner plug was constructed using glass fibre low pH shotcrete which was required to fulfil the following requirements (also mentioned in Chapter 2.2):

- pH of the leached water below 11.7 (in less than 60 days)
- hydraulic conductivity  $K < 10^{-8}$  m/s
- uniaxial strength (cylindrical) minimum 30MPa, recommended 40MPa
- Flexural strength (first peak – at crack creation) minimum 3MPa, recommended 5MPa
- crack size  $< 0.2$  mm; no pass through cracks
- recommended micro silica/cement ratio: 50/50
- minimum amount of fibres  $3 \text{ kg/m}^3$

The outer plug was constructed from shotcrete employing the same procedure as that used for the inner plug; the use of fibres was not compulsory. The same concrete composition was recommended and subsequently used.

##### 4.1.6.2 Concrete composition

The development of a concrete mixture for DOPAS EPSP construction was concluded with the application of low-pH concrete which fulfilled all the required parameters. The detailed “recipe” for the EPSP low-pH concrete mixture and the preparation procedure remain the internal know-how of the subcontractor (conditions set out in the tender were based on pH level requirements; the exact

composition was left to the decision of the supplier with a recommendation with regard to the micro silica /cement ratio).

The composition of the final concrete mixture was as follows (with a microsilica/ cement ratio of roughly 50/50):

- Cement CEM II / B – M (S-LL) 42,5 N
- Sand & gravel 0-4 & 4-8 Dobřín
- Plasticiser SIKA 1035CZ
- Retardant SIKA VZ1
- Accelerator SIKA Sigunit L93 AF
- Microsilica SIKA FUME
- Glass fibres – crack HP (Sklocement Beneš)

#### 4.1.6.3 The testing of the fresh concrete – the settlement and flow table test

This test is important in that it provides for the immediate monitoring of concrete behaviour at the building site following delivery, especially when concrete pumping and spraying is intended. Testing was performed by the subcontractor Metrostav a. s. and the results are available in Myšíčková (2014 and 2015). The “ČSN EN 12350-5 testing of fresh concrete, flow table test” standard was followed. Tests were conducted prior to the installation of both plugs.

The installation of the inner plug took place on 12 – 13 November 2014 at which time concrete samples from each of 6 concrete mixing transport trucks were tested. Settlement results varied between 180 - 260mm and flow values between 350 - 590mm. All the results were deemed acceptable and the concrete was subsequently used for plug construction purposes.

The installation of the outer plug took place on 19 – 20 June 2015 at which time concrete samples from each of 6 concrete mixing transport trucks were tested. Settlement results varied between 250 - 285mm and flow values between 540 - 600mm. All the results were deemed acceptable and the concrete was subsequently used for plug construction purposes.

#### 4.1.6.4 Uniaxial strength

Tests concerning the uniaxial strength of the hardened concrete were performed following the installation of both plugs according to the ČSN EN 12504-1 standard. Testing was performed at the SQZ laboratory and commissioned by the subcontractor Metrostav a. s. Core samples were also examined according to the ČSN EN 12504-1 standard prior to the performance of strength testing (the determination of dimensions; compaction quality – presence and number of pores; distribution of aggregates). Density was determined according to the “ČSN EN 12390-7: the testing of hardened concrete - density of hardened concrete” standard. The results concerning the inner plug (see Tab. 7) are taken from Slanina (2014-a) and those concerning the outer plug from Slanina (2015-a), Tab. 8.

##### Inner plug

Six samples taken following the installation of the inner concrete plug (12 - 13 November 2014) were tested on 10 December 2014 (i.e. after 28 days). The diameter of the samples was around 99mm and their height varied between 109 and 122mm. The results are shown in Tab. 7.

Tab. 7 – Density and uniaxial strength of samples (at 28 day) from the inner plug

Result/ sample	1	2	3	4	5	6	Aver age	Min.
<b>Density (ČSN EN 12390-7) [kg/m<sup>3</sup>]</b>	2205	2204	2211	2186	2205	2210	<b>2200</b>	<b>2186</b>
<b>Uniaxial strength of the core (ČSN EN 12504-1) [MPa]</b>	58.3	56.5	55.3	60.7	52.1	55.3	<b>56.4</b>	<b>52.1</b>
<b>Recalculation of the strength of the cylinder according to ČSN EN 12390-3/Z1 [MPa]</b>	53.1	50.9	49.8	53.4	46.9	50.3	<b>50.7</b>	<b>46.9</b>

The requirements of the tender with regard to the uniaxial strength of the inner plug were at least 30MPa with a recommendation of 40MPa. The average cylindrical value was determined at 50.7MPa and the minimum value revealed by testing 46.9MPa. Thus, all the samples fulfilled and exceeded the recommendation of 40MPa.

### Outer plug

As with the inner plug six samples were taken following the installation of the outer concrete plug (19 June 2015) and tested on 17 July 2015 (i.e. after 28 days). The diameter of the samples was around 99mm and their height varied between 104mm and 106mm. The results are shown in Tab. 8.

Tab. 8 – Density and uniaxial strength of samples from the outer plug

Result/ sample	1	2	3	4	5	6	Average	Min.
<b>Density (ČSN EN 12390-7) [kg/m<sup>3</sup>]</b>	2182	2197	2188	2188	2196	2161	<b>2190</b>	<b>2161</b>
<b>Uniaxial strength of the core (ČSN EN 12504-1) [MPa]</b>	53.0	52.7	55.2	56.3	60.0	53.7	<b>55.1</b>	<b>52.7</b>
<b>Recalculation of the strength of a 150mm cube according to ČSN EN 12390-3/Z1 [MPa]</b>	56.7	56.3	58.8	60.0	63.6	57.4	<b>58.8</b>	<b>53.3</b>
<b>Recalculation of the strength of the cylinder according to ČSN EN 12390-3/Z1 [MPa]</b>	46.1	45.8	48.0	49.0	52.2	46.7	<b>48.0</b>	<b>45.8</b>

The requirements of the tender with regard to the uniaxial strength of the outer plug were also at least 30MPa with a recommendation of 40MPa. The average cylindrical value was determined at 48.0MPa and the minimum value revealed by testing 45.8MPa. Thus, all the samples fulfilled and exceeded the recommendation of 40MPa.

#### 4.1.6.5 Flexural strengths (first peak and ultimate)

Tests on the flexural strength (first peak and ultimate) of beam specimens was also performed following the installation of both plugs according to the “ČSN EN 14488-3: testing of sprayed concrete - flexural strength (first peak, ultimate and residual) of fibre reinforced beam specimens” standard. These tests were also performed by the SQZ laboratory and commissioned by the subcontractor Metrostav a. s. Density was determined according to the “ČSN EN 12390-7: the testing of hardened concrete - density of hardened concrete” standard. The results concerning the inner plug (see Tab. 9) are taken from Slanina (2014-b) and those concerning the outer plug from Slanina (2015-b), Tab. 10.

### Inner plug

Six beam samples were taken following the installation of the inner concrete plug (12 - 13 November 2014) and tested on 10 December 2014 (i.e. after 28 days). The dimensions of the samples were approximately 500 x 126 x 75mm (weight around 10kg). The results are shown in Tab. 7.

Tab. 9 – Density and flexural strengths of samples from the inner plug

Result/ sample	1	2	3	4	5	6	Average	Min.
<b>Density (ČSN EN 12390-7) [kg/m<sup>3</sup>]</b>	2165	2193	2162	2179	2151	2178	<b>2170</b>	
<b>Flexural strength (first peak) [MPa]</b>	5.2	5.4	5.8	6.2	5.7	5.9	<b>5.7</b>	<b>5.2</b>
<b>Flexural strength (ultimate) [MPa]</b>	5.3	5.5	5.9	6.2	5.8	5.9	<b>5.8</b>	<b>5.3</b>

The requirement of the tender with regard to flexural strength (first peak – at crack creation) was a minimum of 3MPa with a recommendation of 5MPa. The average first peak value was determined at 5.7MPa and the minimum value from the test at 5.2MPa. Thus, all the samples exceeded the recommended 5MPa.

## Outer plug

As with the inner plug, six samples were taken following the installation of the outer concrete plug (19 June 2015) and tested on 17 July 2015 (i.e. after 28 days). The dimensions of the samples were approximately 500 x 125 x 76mm (weight around 10.5kg). The results are shown in Tab. 10.

Tab. 10 – Density and flexural strengths of samples from the outer plug

Result/ sample	1	2	3	4	5	6	Aver age	Min.
Density (ČSN EN 12390-7) [kg/m <sup>3</sup> ]	2121	2195	2168	2169	2193	2172	<b>2170</b>	
Flexural strength (first peak) [MPa]	5.5	5.8	5.1	4.5	4.9	5.5	<b>5.2</b>	<b>4.5</b>
Flexural strength (ultimate) [MPa]	5.5	5.8	5.1	4.5	5.0	5.5	<b>5.2</b>	<b>4.5</b>

The requirement of the tender with regard to flexural strength (first peak) was a minimum of 3MPa with a recommendation of 5MPa. The average first peak value was determined at 5.2MPa and the minimum value from the test at 4.5MPa. Thus, all the samples fulfilled the requirement of 3MPa and exceeded or approximated to the recommended 5MPa.

### 4.1.6.6 Hydraulic conductivity

Hydraulic conductivity tests on hardened concrete samples were carried out at the Institute of Geology of the Czech Academy of Science. The results are taken from Petružálek & Nemejovský (2015).

Three samples taken during the installation of the inner concrete plug (12 - 13 November 2014) were tested on 29 December 2014. Cylindrical samples were processed so as to obtain a diameter  $d = 50\text{mm}$  and height  $L = 30\text{mm}$ . The testing procedure followed the “ČSN CEN ISO/TS 17892-11: geotechnical investigation and testing - laboratory testing of soil - part 11: Determination of permeability by the constant and falling head methods” standard. Hydraulic conductivity was determined according to Eq. 1. Subsequently, hydraulic conductivity [m/s] was, according to the standard, recalculated to  $k_{10}$  – value at a water temperature of 10°C. The results are shown in Tab. 11 - Tab. 13. The level of pressure within the testing chamber was maintained at 300kPa and backpressure at around 280kPa (backpressure is equal to the pressure difference related to the hydraulic gradient).

$$k = \frac{V \cdot L}{A \cdot i \cdot t} \quad \text{Eq. 1}$$

- $k$  – hydraulic conductivity [m/s],
- $V$  – water volume [m<sup>3</sup>],
- $L$  – sample height [m],
- $A$  – sample cross-sectional area [m<sup>2</sup>],
- $i$  – difference in pressure heads [m]
- $t$  – time [min]



Figure 23 – Tested samples

Tab. 11 – Hydraulic conductivity parameters - sample P1 ( $k_{10}$  – value at a water temperature of 10°C)

<b>p</b> [kPa]	<b>i</b> [cm]	<b>t</b> [min]	<b>L</b> [mm]	<b>d</b> [mm]	<b>A</b> [cm <sup>2</sup> ]	<b>V</b> [cm <sup>3</sup> ]	<b>T</b> [°C]	<b>k</b> [m/s]	<b>k<sub>10</sub></b> [m/s]
276	2814	5400	30.54	49.95	19.60	3.70	21	6.32E-12	4.76E-12

Tab. 12 – Hydraulic conductivity parameters - sample P2 ( $k_{10}$  – value at a water temperature of 10°C)

<b>p</b> [kPa]	<b>i</b> [cm]	<b>t</b> [min]	<b>L</b> [mm]	<b>d</b> [mm]	<b>A</b> [cm <sup>2</sup> ]	<b>V</b> [cm <sup>3</sup> ]	<b>T</b> [°C]	<b>k</b> [m/s]	<b>k<sub>10</sub></b> [m/s]
287	2927	5235	29.87	49.93	19.58	2.90	21	4.81E-12	3.62E-12

Tab. 13 – Hydraulic conductivity parameters - sample P3 ( $k_{10}$  – value at a water temperature of 10°C)

<b>p</b> [kPa]	<b>i</b> [cm]	<b>t</b> [min]	<b>L</b> [mm]	<b>d</b> [mm]	<b>A</b> [cm <sup>2</sup> ]	<b>V</b> [cm <sup>3</sup> ]	<b>T</b> [°C]	<b>k</b> [m/s]	<b>k<sub>10</sub></b> [m/s]
285	2906	3655	30.12	49.86	19.53	4.10	21	9.92E-12	7.47E-12

*p* – backpressure, *I* - difference in pressure heads, *t* - time, *L* – sample height, *d* – sample diameter, *A* – sample area, *V* – water volume, *T* – temperature during the test, *k* – measured hydraulic conductivity, *k<sub>10</sub>* – hydraulic conductivity recalculated to a value at a water temperature of 10°C.

Hydraulic conductivity (at 10°C) values were found to be in the range  $k_{10} = 3.6 - 7.5E-12$  m/s which indicated the same order of magnitude as the required and real values with regard to the bentonite pellet sealing section.

The rock surrounding the EPSP experiment was sealed using grouting to a distance of 5m from the original excavation and the resulting hydraulic conductivity of the rock mass was subsequently tested ( $<10^{-10}$  m/s) (D3.20 Installation report, Svoboda et. al., 2016). All the values with concern to the concrete plugs are approximately one order of magnitude better, i.e. less permeable.

The requirement of the tender with concern to concrete was  $k = 10^{-8}$  m/s and better; therefore, it can be concluded that the concrete exhibits the required behaviour.

#### 4.1.6.7 pH leachate

The testing of pH leachates was performed at ÚJV Řež a. s. and commissioned by the subcontractor Metrostav a. s. The results (see Tab. 14) are taken from Večerník (2015). Three samples taken during the installation of the inner concrete plug (12 - 13 November 2014) were tested on 29 December 2014. The cement material pH leachate measurement procedure was based on the SKB R-12-02 report (Alonso et al., 2012). The cement/concrete samples were hardened for 28 days following which the samples were finely ground and mixed together with de-gassed distilled water (ratio 1:1); pH values were then measured in suspension and in the filtrated liquid. The measurement of pH takes only several minutes and should, ideally, be performed in an inert atmosphere (e.g. N<sub>2</sub>) so as to avoid the influence of CO<sub>2</sub> dissolution and interaction in the liquid phases; however, an inert atmosphere was not used in this case.

Tab. 14 – pH results

Sample	pH of suspension	Average pH of suspension	pH of filtrate	Average pH of filtrate
PH1	11.42	11.4	11.32	11.3
	11.38		11.31	
	11.39		11.31	
PH2	11.35	11.4	11.28	11.3
	11.36		11.30	
	11.38		11.31	
PH3	11.39	11.4	11.28	11.3
	11.38		11.28	
	11.40		11.29	

The tender documentation set out the requirement with regard to the pH of concrete leachates of 11.7 and lower. Since the average values are 11.3 and maximum values 11.4 none of the tests exceeded the limit; thus the concrete fulfilled the given requirements.

#### 4.1.6.8 Thermo-physical parameters

The determination of thermal conductivity and heat capacity was conducted by the CEG by means of an ISOMET 2114 device on cylindrical samples taken during the installation of the inner plug. The device and testing procedure were the same as used for the bentonite samples; a surface probe was used for which a flat surface of at least 60mm in diameter is sufficient. The demand for the accuracy of surface flatness increases with the increasing thermal conductivity value of the tested material. The expected minimum thickness of the evaluated material ranges from 20mm to 40mm depending on its diffusivity (conductivity). (Applied precision, 2014)

Based on both information provided from the producer of the device and own experience it was decided that cylindrical samples ( $d = 100\text{mm}$ ,  $h = \text{approximately } 100\text{mm}$ ) would be sufficient. A sequence of three measurements was conducted on each of eight measured positions on both bases. The results are provided in Tab. 15.

Tab. 15 – Thermal conductivity and heat capacity

No. of tests: 24	w	$\rho_d$	$\rho$	$\lambda$	$c_p$	a	c
	%	kg/m <sup>3</sup>	kg/m <sup>3</sup>	W/m.K	[J/m <sup>3</sup> K] x10 <sup>-6</sup>	[m <sup>2</sup> /s] x10 <sup>-6</sup>	[J/kg.K]
Average value	8.00	2030	2192	2.03	1.83	1.11	837
Standard deviation				0.08	0.08	0.03	37
Coefficient of variation				0.04	0.04	0.03	0.04

w – water content,  $\rho_d$  – dry density,  $\rho$  – density,  $\lambda$  - thermal conductivity, a - thermal diffusivity,  $c_p$  – volume heat capacity, c – heat capacity

Thermo-physical properties are important in cases where heat transfer is anticipated. This is not the case in terms of the main testing aims of the EPSP experiment; however, it will be necessary to have a knowledge of such parameters in relation to the future deep repository. Moreover, heat is generated during the concrete hydration process. Therefore, tests were carried out so as to provide material parameters which will allow the potential accurate modelling of EPSP behaviour. No limit values were set either for thermal conductivity or heat capacity. A comparison of the thermal conductivity of concrete and bentonite is shown in Figure 24.

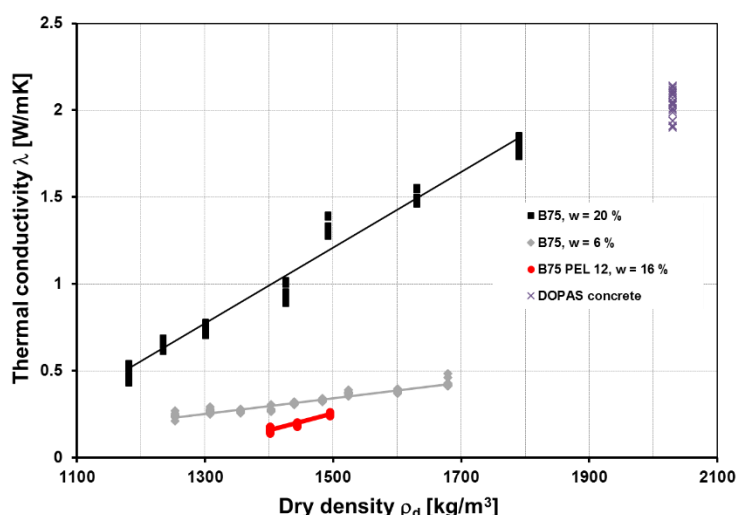


Figure 24 – Thermal conductivity of the bentonite samples and concrete

The thermal conductivity values of the concrete are significantly higher than those of the bentonite pellets at a density of the same level as in the EPSP sealing section. As can be seen from *Figure 24*, almost saturated highly-compacted bentonite blocks have the potential to attain similar values as those of concrete.

#### **4.1.7 Conclusion regarding the work conducted by the CEG-CTU**

The CTU laboratory research was undertaken as a supporting activity for the construction of the EPSP experiment. The basic laboratory tests performed by the CTU initially focused on the estimation of the specific density and Atterberg limits of the bentonite powder. This was followed by the determination of hydraulic conductivity and swelling pressure with regard to compacted samples (several dry density values).

The input/ initial laboratory testing of the bentonite was completed as planned in D 3.16, i.e. the verification testing of hydraulic conductivity and swelling pressure on bentonite pellets continued until mid-2015 (mixtures as used in the bentonite section of the EPSP). However, the most important “laboratory” tests performed by the CTU were those which focused on the manufacture of the pellets, compaction (field) tests and shot clay (sprayed bentonite) technology.

B75 is produced in powder form, which is not ideal for sealing purposes due to its low level of compaction. Therefore, the testing of the most appropriate technology for the manufacture of the pellets, in cooperation with potential Czech producers, was also carried out by the CTU. The main conclusion from this research is that pellets from B75\_2013 bentonite demonstrated sufficient dry density levels and, therefore, can be considered as meeting the various requirements pertaining to the geotechnical behaviour of the bentonite seal in the EPSP experiment.

In addition, various potential technologies with regard to bentonite emplacement were tested. Based on the results of these tests and on the very limited time available for bentonite application, the use of ice was ruled out. Following the fine tuning of alternative application machinery, it was possible to achieve the same deposited material density using sprayed bentonite pellets only (at a much higher application speed).

In-situ sampling was conducted during the construction of the EPSP bentonite sealing section so as to monitor the achieved dry density of the pellet layer. Requirements pertaining to dry density ( $1.4\text{Mg/m}^3$ ) were fulfilled with regard to the whole volume of the seal.

Responsibility for the verification testing of concrete quality during and after construction was accorded to CTU subcontractor Metrostav a. s. The specific requirements concerning tests on concrete samples were set out in the public tender documentation. During negotiations on the initial contract, some changes in testing plan were agreed to provide for the improved monitoring of both fresh and hardened concrete. Testing included the flow table test and tests aimed at the determination of uniaxial and flexural strength, hydraulic conductivity and leachate pH. It can be concluded that all the parameters tested by CTU fulfilled the required criteria.

## 4.2 Work performed by SÚRAO

### 4.2.1 Mineralogical composition of the bentonite

The bentonite pellet zone is comprised of “Bentonit 75” bentonite, a natural and high-smectite-content Ca-Mg bentonite with notably high iron content in the octahedral layer of the smectite. The purpose of the bentonite is to seal and absorb/adsorb any water that leaks across the inner concrete plug. The bentonite zone is 2-m long. The mineralogical and chemical composition of bentonite B75\_2013 (batch from 2013) is presented in *Figure 25* and in *Tab. 16*.

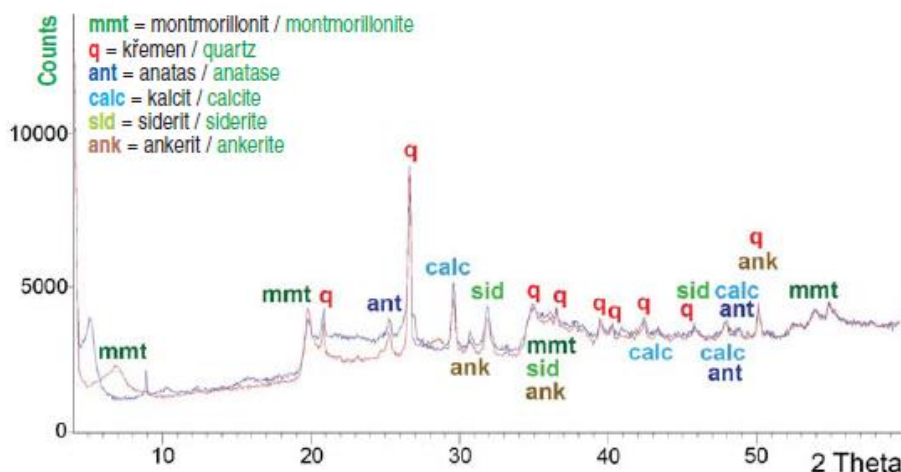


*Figure 25 - X-ray diffraction pattern B75\_2013 (X'Pert PRO, CuK $\alpha$ , 40 kW, 30 mA, High Score Plus, analysed by the University of Chemical Technology, red spectrum – sample B 75\_2013, blue spectrum – the same sample after glycolation)*

*Tab. 16 - Silicate analysis of bentonite B 75\_2013 (weight percentage)*

	hm. %
SiO <sub>2</sub>	49,83
Al <sub>2</sub> O <sub>3</sub>	15,35
TiO <sub>2</sub>	2,82
Fe <sub>2</sub> O <sub>3</sub>	10,9
FeO	3,74
MnO	0,09
MgO	2,88
CaO	2,01
Na <sub>2</sub> O	0,67
K <sub>2</sub> O	1,05
P <sub>2</sub> O <sub>5</sub>	0,63
CO <sub>2</sub>	3,66

### 4.2.2 Filling of the fissures in the rock massif

The detailed mineralogical study of the fillings of fissures was carried out in niche SP-59 in 2013; the sampling locations are shown on the map in *Figure 26*. Six samples were analysed by means of X-ray powder diffraction at the Institute of Chemical Technology, Prague, VŠCHT (X'Pert PRO with Bragg-Brentan geometry, CuK $\alpha$ , 40kV, 30mA, High Score Plus) and SEM at the Faculty of Science, Charles



## 4.2.3 In-situ tests

### 4.2.3.1 Water pressure tests of the rock mass

Water pressure tests (WPT) were conducted for the purpose of the checking of the grouting of the rock mass in the space intended for the construction of the plug. A total of six boreholes 76mm in diameter and 3.1m long were drilled so as to verify the sealing capacity of the rock mass up to a depth of 5m. An additional four boreholes 14mm in diameter and 0.3m long were drilled for the verification of the sealing capacity of the near-surface layer of the rock massif in the space intended for the outer plug (See Figure 27). Water pressure testing was conducted both prior to and following the injection of the grouting material. Position of the boreholes can be seen on Figure 28 and Figure 29. Drills are marked as VTZ.



Figure 27 – Water pressure testing in the near-surface layer

Once the testing procedure had been completed, the longer boreholes were filled using WEBAC 1660 resin.

Water pressure testing was performed in the VTL-2 horizontal verification borehole. Once a test pressure level of 2MPa had been attained, it was verified that the hydraulic parameters ranged from  $3.81\text{E-}9$  to  $7.71\text{E-}9\text{m/s}$ . After exceeding 2MPa, an exponential increase in the consumption of test water was observed (see *Tab. 17*, Figure 30 and Figure 31) and effluents were detected on the surface of the niche (Sosna et al., 2014b). (Water consumption was reading from the suction side of the pump in a the measurement container with nominal diameters 13,1x 8.4 cm. Water consumption was read for 1.0 min for 10 min at stable consumption.)

After attaining a test pressure level of 2MPa in the VTZ-3 and VTZM-1 horizontal verification boreholes, it was verified that the hydraulic parameters in the rock massif following injection ranged from  $1.24\text{E-}10$  to  $2.49\text{E-}10\text{m/s}$  (See *Tab. 18*).

Finally, the VTZ-4, 5, 6 and VTZM-2, 3, 4 ceiling verification boreholes were also subjected to test pressures of up to 2MPa and it was verified that the hydraulic parameters in the rock massif following injection ranged from  $1.79\text{E-}9$  to  $2.58\text{E-}10\text{m/s}$  (*Tab. 19*).

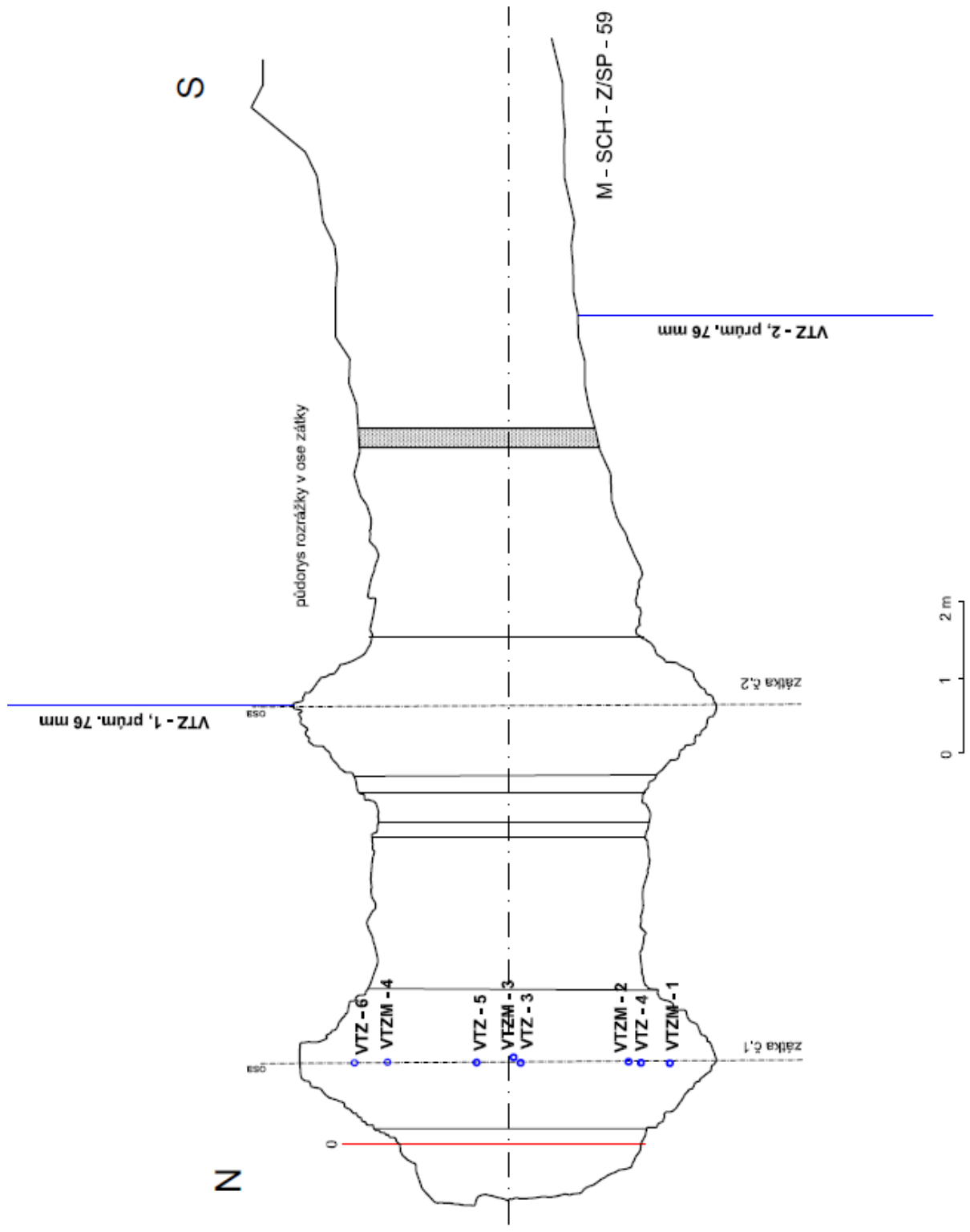


Figure 28 – Position of boreholes for hydraulic tests (VTZ), horizontal section, SP-59 (Malý, 2015)

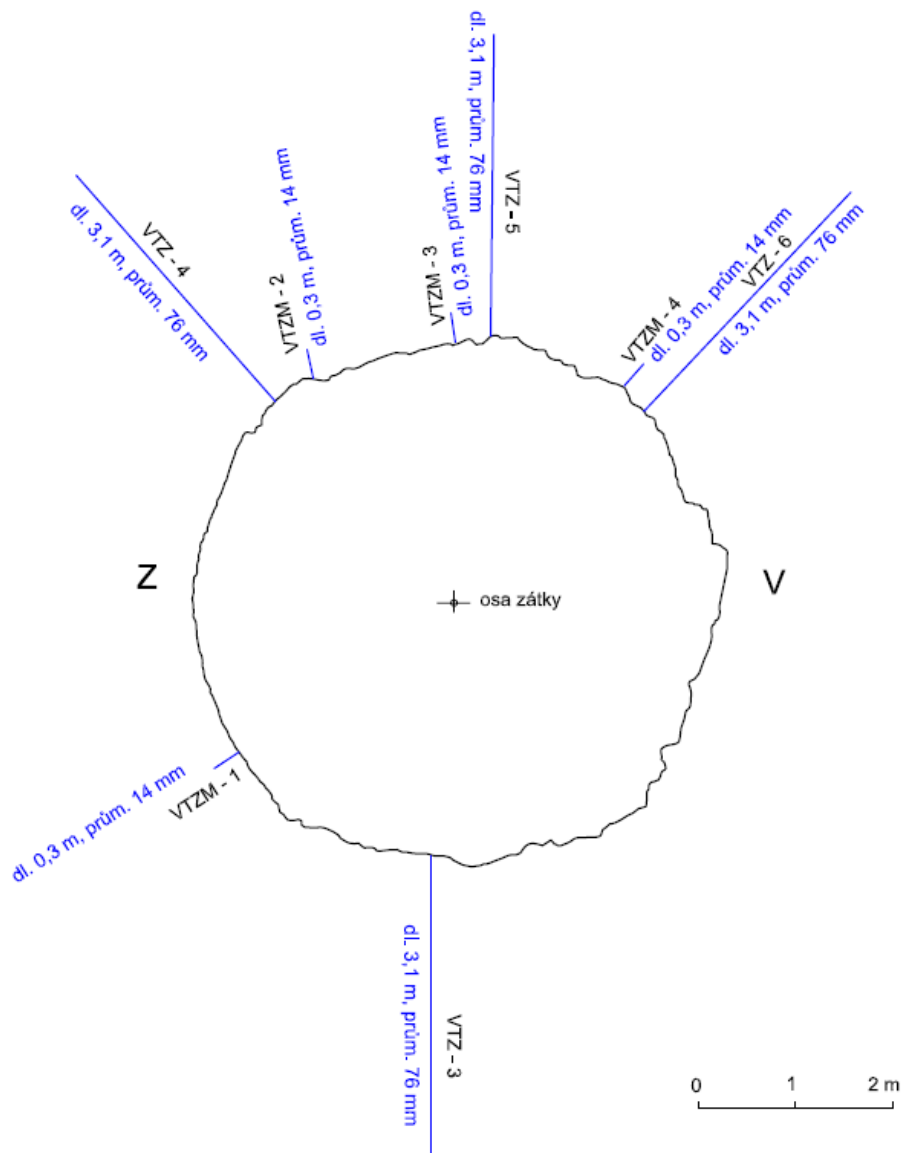


Figure 29 – Position of boreholes for hydraulic tests (VTZ), vertical section 1.1m from the face, SP-59 (Malý, 2015)

Tab. 17 - Water pressure test VTZ-2 (Sosna et al., 2014b).

WPT VTZ-2	Time (min)	(cm)	Q (m <sup>3</sup> /s)	k (m/s)
Level		Reading consumption	Water consumption	Hydraulic conductivity
1.25-4.5	11	9.8	1.63E-06	3.81E-09
1.25-4.5	9	32.5	6.62E-06	7.71E-09
1.25-4.5	5	45.5	1.67E-05	1.30E-08
3.0-4.5	10	9.8	1.80E-06	7.59E-09
3.0-4.5	10	13.1	2.40E-06	5.08E-09
3.0-4.5	4	24	1.10E-05	1.55E-08
3.0-4.5	0.5	24.7	9.06E-05	9.57E-08

Tab. 18 - Water pressure test VTZ-3 (Sosna et al., 2014b).

WPT VTZ-3	Time (min)	(cm)	Q	k
			(m <sup>3</sup> /s)	(m/s)
Level		Reading consumption	Water consumption	Hydraulic conductivity
1.13-3.1	4	0.0	0.0	Could not be evaluated - impermeable
1.13-3.1	30	0.1	1.45E-07	2.49E-10
1.13-3.1	30	0.05	7.23E-08	1.24E-10

Tab. 19 - Water pressure tests in boreholes VTZ-4, 5, 6 and 2, 3, 4-VTSM (Sosna et al., 2014b).

WPT	Time (min)	(cm)	Q	k
			(m <sup>3</sup> /s)	(m/s)
Level		Reading consumption	Water consumption	Hydraulic conductivity
<b>VTZ4</b>				
1.24-3.05	14	0.1	3.10E-07	5.57E-10
<b>VTZ5</b>				
1.24-3.1	10	0.1	4.34E-07	7.80E-10
<b>VTZ6</b>				
1.24-3.12	15	0.05	1.45E-07	2.58E-10
<b>VTSM-2</b>				
0.13-0.31	10	0.05	2.17E-07	1.79E-09
<b>VTSM-3</b>				
0.13-0.29	10	0	N/A	
<b>VTSM-4</b>				
0.13-0.295	10	0	N/A	

VTL-2 etáž 1,25 - 4,5 m

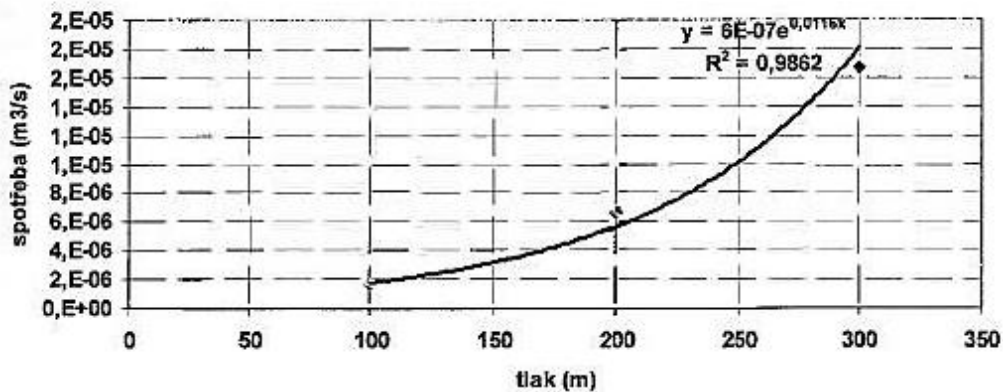


Figure 30 - Dependence of consumption water on test pressure VTL-2 level 1,25-4,5m

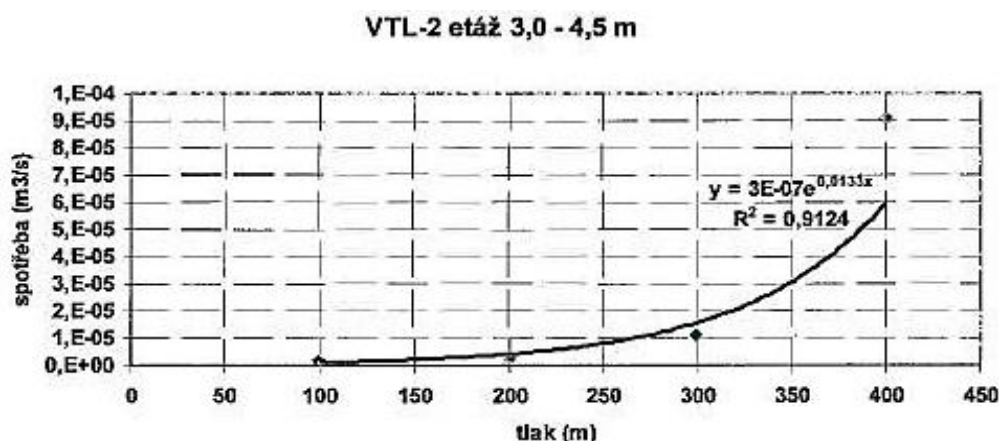


Figure 31 - Dependence of consumption water on test pressure VTL-2 level 3,0 – 4,5m

#### 4.2.3.2 Goodman- Jack uniaxial press tests

Goodman-Jack uniaxial press tests were performed in the VTZ-2 borehole with a diameter of 76mm and a length of 4.5m. Tests were conducted at eight incremental depth levels between 0.8m and 4.3m at 0.5m intervals employing alternately the horizontal and vertical rotation of the jaws of the test press. The tests were performed using the Goodman-Jack apparatus – Hard Rock type.

Stepped load increments were chosen of 5MPa to 20MPa, with strain values at the same step value of 5MPa for all the increments and, subsequently, the second cycle was loaded with the same steps until a maximum value of 40MPa had been attained (Sosna et al., 2014a).

The results of the modulus of elasticity ( $E_p$ ) and deformation ( $E_{def}$ ) tests in borehole VTZ-2 are presented in Tab. 20:

Tab. 20 - Modulus of elasticity ( $E_p$ ) and deformation ( $E_{def}$ ) tests in borehole VTZ-2 (Sosna et al., 2014b).

Orientation of the jaws	Depth (m)	$E_{def,1}$ GPa	$E_{def,2}$ GPa	$E_{def,2all}$ GPa	$E_{p,1}$ GPa	$E_{p,2}$ GPa	$E_{p,2all}$ GPa
		5-20 MPa	20-40 MPa	5-40 MPa	20-5 MPa	40-20 MPa	40-5 MPa
Horizontal	0.8	8.1	10.9	10.0	8.6	13.9	10.4
	1.8	3.8	8.2	6.8	5.3	14.6	7.8
	2.8	10.0	14.3	11.9	10.0	17.8	12.7
	3.8	2.3	5.4	4.5	3.4	16.5	5.0
Vertical	1.3	5.1	9.8	8.7	7.1	15.6	9.7
	2.3	5.3	14.2	13.9	11.9	20.0	14.1
	3.3	7.6	9.4	10.0	11.9	15.1	11.0
	4.3	10.8	14.3	13.1	13.1	16.6	13.1

#### 4.2.4 Static plate test

Further tests were conducted directly inside the space for the plug in niche SP-59. The static plate test for determining the modulus of deformation was carried out on the axis of inner plug, at the bottom of the excavation. The resultant modulus of deformation is 5-10GPa and modulus of elasticity 15-17GPa (Filala et al., 2014).

#### 4.2.5 Laboratory tests

Laboratory tests were conducted for the determination of bulk density, strength in transverse tension, unconfined compression strength and modulus of deformation  $E_{def}$  (MPa). The tests were carried out on specimens of the rock mass (tonalite in SP-59). Six 50mm-diameter specimens with a slenderness ratio of 1:2 were analysed. The laboratory tests were performed at the ARCADIS CZ a.s. accredited laboratory, Tab. 21 (Záruba, 2015).

Tab. 21 - *Laboratory determination of the modulus of elasticity, deformation, unconfined compression strength and strength in transverse tension - average values taken from six analysed samples (Filala et al., 2014)*

<i>Compression strength (MPa)</i>	<i>Strength in transverse tension (MPa)</i>	<i>Modulus of elasticity (GPa)</i>	<i>Modulus of deformation (GPa)</i>
121.78	8.4	79.94	79.98

#### 4.2.6 Conclusion regarding the work conducted by the SÚRAO

The rock massif around the EPSP experiment was improved by means of grouting using polyurethane resins. Following injection, the rock mass demonstrated significantly lower values of permeability. This was later confirmed by the results of water pressure testing (see *Tab. 17 - Tab. 19*). Other measurements taken of the various geotechnical parameters concerned the overall conditions of the rock mass (see *Tab. 20* and *Tab. 21*).

As a result of the successful construction of the EPSP experiment, the first objective (the demonstration of the suitability of the technology) of the DOPAS EPSP experiment has been achieved. “Alternative” technologies (such as shotcreting, shotclay application and GBT) and materials (low pH shotcrete, bentonite pellets) have been successfully tested.

### 4.3 Work performed by the ÚJV Řež, a. s.

#### 4.3.1 Laboratory tests on bentonite

The material used for the construction of the plugs and the laboratory physical models as well as for further testing consists of commercially produced Bentonit 75 (B75) supplied by KERAMOST, Plc., Czech Republic. This product follows on from the materials studied in previous research focused on barrier materials for deep geological waste repositories, the parameters of which are described in a report (in Czech only) entitled: “Shrnutí informací o vlivu chemického složení bentonitu Rokle na chemické a fyzikální vlastnosti” - Summary information on the effect of the chemical composition of Rokle bentonites on chemical and physical properties.

As a consequence of the use of B75 in various industrial sectors, the material is subjected to laboratory testing on a continuous basis in terms primarily of changes both in its mineralogical and chemical composition and physical properties. Experiments focus principally, in addition to the study of chemical and mineralogical composition, on leachate analysis, the determination of ion-exchange capacity etc. The data obtained to date forms part of the Czech report.

*The results of an internal report concerning those bentonites to be employed in the construction of the plug can be summarised as follows: a literature survey revealed that minor differences exist between two local sources of bentonite in the Czech Republic, i.e. the Doupovské hory volcanic region (main deposit Rokle) and the České středohoří volcanic region (main deposit Braňany - Černý vrch) (Franče, 1992). Several significant differences can be detected via a visual inspection of raw bentonite samples, while a number of minor differences have been identified following the study of chemical composition (especially in terms of the total amount of sodium, potassium and calcium). Nevertheless, the mineralogical composition and crystal chemistry of the bentonites from these two sources as well as the amount of montmorillonite present are very similar, as reported by Franče (1992). Currently, factory-produced bentonite Bentonit 75 (B75) is slightly different from previously studied bentonites extracted from the Rokle deposit (raw samples as well as factory-produced B75) - see Tab. 22 which provides a comparison of the chemical analysis of bentonite B75\_2010 produced in 2010 (and used in previous projects) and bentonite B75\_2013 produced in 2013 and used in this project. The testing of the production of pellets was performed using B75\_2013 (by the CEG). It is assumed that differences identified in the properties of the two materials (free swelling, ionic form, pH of the suspension) are the result of the processing technology employed and/or the different source of the raw bentonite (different deposit or a different part of the same deposit). A comparison of the leachate pH of these two materials in distilled water is provided in Tab. 23 which provides the suspension pH results for different solid/liquid ratios after 28 days of exposure. Analyses of leachates of B75 in distilled water were performed for bentonite samples from both 2010 and 2013 with differing solid/liquid ratios. As can be seen in Tab. 24, the concentration of Na<sup>+</sup> in B75\_2013 leachates is significantly lower than in B75\_2010.*

The processing technology has been identified as the main factor affecting the properties of B75 produced in recent years. Further, it was found that partial activation and/or contamination caused by the presence of an activation reagent affect the composition of the water suspension or water leachate, cation exchange capacity and bentonite pore water composition. The chemical composition of the B75\_2013 (the material chosen for the verification of selected parameters) sample was found to be different from samples studied previously – especially in terms of the amount of total sodium, calcium, iron and carbon/carbonates (see Tab. 22).

Tab. 22 - Chemical analysis of bentonite B75; comparison of materials produced in 2010 (B75\_2010) and 2013 (B75\_2013)

wt%	B75_2010	B75_2013
SiO <sub>2</sub>	51.91	49.83
Al <sub>2</sub> O <sub>3</sub>	15.52	15.35
TiO <sub>2</sub>	2.28	2.82
Fe <sub>2</sub> O <sub>3</sub>	8.89	10.9
FeO	2.95	3.74
MnO	0.11	0.09
MgO	2.22	2.88
CaO	4.60	2.01
Na <sub>2</sub> O	1.21	0.67
K <sub>2</sub> O	1.27	1.05
P <sub>2</sub> O <sub>5</sub>	0.40	0.63
CO <sub>2</sub>	5.15	3.66

Tab. 23 – pH values of the B75 leachate; comparison of materials produced in 2010 (B75\_2010) and 2013 (B75\_2013) at different solid/liquid (s/l) ratios, contact time: 28 days

s/l ratio	B75_2010	B75_2013
18.6g/l	9.65	9.52
125g/l	9.34	9.22

Tab. 24 – Chemical analysis of B75 leachates - concentrations of major cations. Comparison of materials produced in 2010 (B75\_2010) and 2013 (B75\_2013) at different solid/liquid (s/l) ratios

	s/l ratio	18.6g/l	27.9g/l	37.2g/l	62.5 g/l	100g/l	125g/l
	c (mg/l)						
B75_2010	Na <sup>+</sup>	93	96	132	190	255	260
	K <sup>+</sup>	5.6	7.0	7.9	10.8	11.6	11.6
	Mg <sup>2+</sup>	0.54	0.88	1.10	1.70	2.20	2.90
	Ca <sup>2+</sup>	1.91	1.94	2.07	2.19	2.06	2.77
B75_2013	Na <sup>+</sup>	57.9	80.1	85	81.7	123.7	123.5
	K <sup>+</sup>	8.7	9.3	9.1	8.0	12.4	12.6
	Mg <sup>2+</sup>	3.7	2.5	2.4	3.3	4.1	3.6
	Ca <sup>2+</sup>	1.8	2.1	2.5	2.9	3.4	2.7

#### 4.3.1.1 Hydraulic conductivity tests

The laboratory equipment to be used for hydraulic conductivity testing purposes was successfully verified by means of a preliminary test on a specimen of saturated bentonite. The initial testing of a bentonite sample with a dry density of 1.2g/cm<sup>3</sup> and an applied water pressure gradient of 4 bar revealed a hydraulic conductivity value of  $\sim 3.6 \cdot 10^{-12}$  m/s.

A test set of samples of powdered B75\_2013 bentonite compacted to 1.4g/cm<sup>3</sup> was subsequently prepared for further study. This compaction value represents the (lower) limit dry density of the material which it is supposed will be achieved by both spray technology and the compaction of the bentonite pellets and powder for the construction of the plug in situ. The pressure range was determined on the basis of the permeability testing of the grouted rock in the plug construction niche and the highest input water pressure was set at 2MPa. The values of the permeability/hydraulic conductivity of the bentonite

material will influence the nature and functionality of the EPSP experimental plug. The laboratory values obtained will be used for the purposes of comparison with the behaviour of the experimental plugs in situ and the verification of numerical models describing the plug in WP5.

Experiments were conducted on two types of experimental sample hereinafter referred to as "small cell/small samples" and "large cell/large samples" in the text. The interior dimensions of the experimental cells consisted of:

- small cell: diameter 30mm and length 15mm
- large cell: diameter 80mm and length 50mm.

Since the size of the bentonite pellets did not allow their placement in the small cells, bentonite pellets were used for large experimental cell purposes only. In order to further approximate to the real conditions under which the experiment was being conducted, synthetic granitic water (Havlová, 2010) was used in the EPSP laboratory tests. The maximum pressure applied in the experiments was 2.0MPa.

### Small cells

Experiments were performed in small cells aimed at the study of the permeability of compacted powdered bentonite B75. The material was compacted into the experimental cells so as to attain a dry density value of 1400kg/m<sup>3</sup> and subsequently fully saturated with synthetic granitic water. Following saturation, hydraulic conductivity tests were performed and the results are summarised in Tab. 25. The experiments were performed with input water pressure values of 1.6MPa and 2.0MPa. Hydraulic conductivity coefficient values were subsequently calculated from the resulting data with a constant steady flow of water through the sample - from the linear part of the curve (see Figure 32).

Tab. 25 - Hydraulic conductivity of the small samples

powdered B75	dry bulk density (kg/m <sup>3</sup> )	input water pressure (MPa)	hydraulic conductivity (m/s)
A1-16	1400	1.6	$5.24 \cdot 10^{-13}$
B1-16	1400	1.6	$4.78 \cdot 10^{-13}$
A2-16	1400	1.6	$5.24 \cdot 10^{-13}$
B2-16	1400	1.6	$4.87 \cdot 10^{-13}$
A1-20	1400	2.0	$4.94 \cdot 10^{-13}$
B1-20	1400	2.0	$4.77 \cdot 10^{-13}$
A2-20	1400	2.0	$5.70 \cdot 10^{-13}$
B2-20	1400	2.0	$5.40 \cdot 10^{-13}$

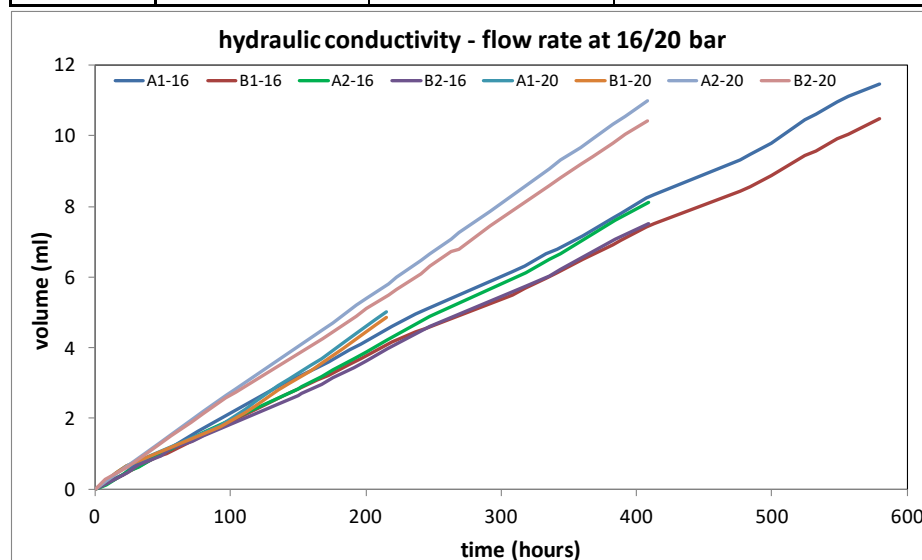


Figure 32 - Hydraulic conductivity tests of B75 small samples - water flow rates

### Large cells - bentonite pellets

The same pellets as those used in the construction of the EPSP were used for determining the hydraulic conductivity of the compacted bentonite pellets. The pellets were compacted into the large cells so as to attain a final dry bulk density value of  $1400\text{kg/m}^3$ . The densities of the bentonite samples were calculated according to the volume of the experimental cells and the dry weight of the pellets. The samples thus prepared were then saturated by means of synthetic granitic water and, following saturation, were connected to a water supply which provided a cell input water pressure of 2.0MPa. The quantity of water flow through the sample was recorded throughout the duration of the experiment (see Figure 33) and coefficients of hydraulic conductivity were calculated from the linear parts of the curves (Tab. 26). Experiments were performed three times on three samples; the application pressure was 2MPa in all cases.

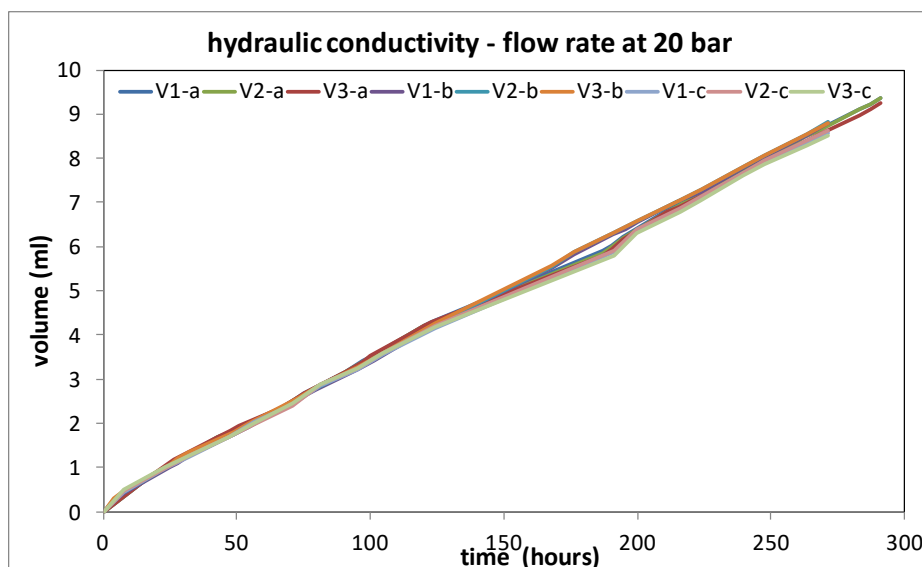


Figure 33 - Hydraulic conductivity tests on B75 pellets in large cells- water flow rates

Tab. 26 - Hydraulic conductivity of B75 pellets in large cells

B75 pellets	dry bulk density ( $\text{kg/m}^3$ )	input water pressure (MPa)	hydraulic conductivity (m/s)
V1-a	1400	2.0	$3.20 \cdot 10^{-13}$
V2-a	1400	2.0	$3.19 \cdot 10^{-13}$
V3-a	1400	2.0	$3.16 \cdot 10^{-13}$
V1-b	1400	2.0	$3.22 \cdot 10^{-13}$
V2-b	1400	2.0	$3.23 \cdot 10^{-13}$
V3-b	1400	2.0	$3.22 \cdot 10^{-13}$
V1-c	1400	2.0	$3.14 \cdot 10^{-13}$
V2-c	1400	2.0	$3.16 \cdot 10^{-13}$
V3-c	1400	2.0	$3.12 \cdot 10^{-13}$

#### 4.3.1.2 Gas permeability tests

Document D3.16 (Vašíček et al., 2013) made mention of gas permeability measurements. The first physical models employing bentonite pellets revealed that the voids surrounding the pellets are

continuous and that water and thus air freely permeate up to the time that the pellets swell to form a fully homogeneous material.

However, an input parameter study was performed on the bentonite employing gas permeability tests. Bentonite powder was compressed to reach various dry bulk densities and saturated in an experimental cell (diameter: 30mm, length: 15mm). One side of the cell was connected to a gas source which allowed a gradual increase in pressure and the second side was connected to a water reservoir. The gas pressure was increased continuously until gas breakthrough was observed (in the form of bubbles in the water reservoir). The average values of breakthrough pressure for various bentonite densities are shown in Tab. 27.

Tab. 27 - Gas breakthrough pressures for saturated bentonite at different dry bulk densities

bentonite dry bulk density (kg/m <sup>3</sup> )	Gas breakthrough pressure (MPa)
1200	5.5
1400	8.0
1600	10.0

#### 4.3.2 Laboratory tests on grouting materials

Before the construction of the plug could commence it was deemed necessary to grout the surrounding rock so as to reduce the permeability of the rock mass to an appropriate level. However, it was thought that interaction with the various alkaline solutions released from the concrete barrier of the plug might lead to the degradation of the grouting material and thus affect the mass of the grouted rock. Thus, the polyurethane-based grouting materials employed by the subcontracting company in the Josef gallery were tested in the team's laboratories.

The first type of test studied the interaction of grouting material with alkaline fluids simulating ordinary cement leachates. The samples were immersed in solutions of alkalis synthetic granitic water (pH up to 13) and monitored over the long term. The results revealed that the extent of interaction of the grouting material and alkaline solutions was minimal and had no visible effect either on the nature or the structure of the grouting material (D3.17).

The second procedure consisted of the permeability test. The middle part of experimental cell was filled with a polyurethane grouting material which was allowed to stabilise (see Figure 34). Subsequently, synthetic granitic water was gradually applied up to a pressure of 2.5MPa. No flow through the sample was observed.



Figure 34 - Sample of a polyurethane-based grouting material subjected to the permeability test.

### 4.3.3 Laboratory tests on the concrete/cement

#### 4.3.3.1 pH measurements

One of the most important quantities of the concrete materials used in the construction of the plug consisted of the pH value of the extract/leachate. One of the requirements of the concrete mixture was that it should be "low-pH concrete" which generally indicates extract pH values of  $\sim 11.5$  or less. The recommended procedure for the pH determination of low-pH leachates from concretes is described in the SKB R-12-02 report: "the Development of an accurate pH Measurement Methodology for the Pore Fluids of low pH cementitious Materials (Alonso et. al., 2012). The ÚJV's previous experience with the preparation of low pH leachate cement mixtures and the experience of a commercial producer of concrete mixtures for building purposes were both employed when determining the first proposal for the concrete mix composition for the construction of the concrete parts of the experimental plug. The cement mixture formerly developed by the ÚJV achieved a pH level of  $< 11$  in the leachate. Two types of cement were used for the development of low-pH cement mixtures: CEM III/B (CEM III/B 32.5 N-SV – Heidelberg) and CEM II 42.5R (CEM II A-S 42,5R – Lafarge) mixed together with a silica fume (Addiment Silicoll P), fine milled limestone (D8 – Lhoist) and a plasticiser (Addiment FM 935). In comparison, the pH of selected commercially-produced materials was determined at pH  $\sim 12$  (see Tab. 28). Although the mixtures developed by the ÚJV exhibit low pH leachates, they are unsuitable for practical use in construction projects due to their low compressive strength. All the cement/concrete pH testing was performed using distilled water. A reduction in the pH of the cement mixture leachate can be obtained by the partial replacement of the cement by another type of binder; it can also be modified by increasing the ratio of fine  $\text{SiO}_2$  (microsilica/silica fume) to the cement content. A study of leachate pH changes for cement mixtures with the partial replacement of the cement with metakaolin was prepared in cooperation with the CEG CTU. The measured pH values of mixtures tested with the partial substitution of cement with metakaolin are presented in D3.17. The substitution of the binder with metakaolin was found to result in a decrease in pH from 13.1 to 11.9. It can be seen that the replacement of cement with metakaolin significantly reduced the pH of the extracts after just 1 month of cement mixture ageing. However, the negative influence of the addition of metakaolin to the cement mixture lies in its possibly leading to a decrease in strength; while this parameter has not yet been tested, the behaviour of samples in powder form prepared for the analysis of pH would seem to indicate that a decrease in compressive strength can indeed be expected.

The replacing of part of the cement in the mixture with  $\text{SiO}_2$  led to the development and testing of several mixtures. Testing revealed that increasing the  $\text{SiO}_2$  content in the mixture (ratio: cement/ $\text{SiO}_2 = 1/1$ ) leads to a decrease in the pH value of the leachate to  $\sim 11.5$  (Vašíček et al., 2014) after 28 days of hardening and fulfils the required limit for the concrete used in EPSP construction. According to information available on practical experience presented at a recent project meeting, pH values decrease after a longer time period than 28 days which was not considered sufficient for the full development of the chemistry of the mixture. A revision of the information suggested that a decrease in pH should be expected within a period of six weeks or longer. This will be confirmed following the dismantling and subsequent evaluation of a physical interaction model in which the concrete will be allowed to age.

Ongoing cooperation with the subcontractor led to the development of low-pH concrete achieving all the required parameters (pH, compressive strength, applicability in situ etc.). Several laboratory samples were prepared based both on ÚJV laboratory experience with the preparation of laboratory-scale mixtures and their subsequent chemical characterisation and analysis and subcontractor experience with the technology and real-scale preparation of concrete mixtures. The final two "recipes" were subjected to testing for the purposes of the application of spraying technology in the test niche as well as for the evaluation of their physical and chemical (leachate pH) properties. The development of a concrete mixture for DOPAS EPSP construction was completed with the application of low-pH concrete with the required parameters (leachate pH = 11.4). The exact recipe for the preparation of the EPSP low-pH concrete mix remains the internal know-how of the subcontractor.

Tab. 28 - Comparison of the pH leachate values of various types of cement and concrete mixes. Mixture T-22, T-23 and P-1 were developed by ÚJV, mixtures S-1 and S-2 (repetition of S-K-1 and S-K-2) make up samples from selected commercially-produced concretes

sample	pH - suspension	average pH	pH - filtrate	average pH
T-22	10.94	10.9	10.78	10.8
	10.88		10.80	
	10.89		10.79	
T-23	10.83	10.8	10.75	10.8
	10.80		10.76	
	10.79		10.76	
S-1	11.91	11.9	11.94	12.0
	11.93		11.96	
	11.89		11.96	
S-2	11.93	12.0	11.94	11.9
	11.95		11.95	
	11.98		11.93	
S-K-1	11.85	11.8	11.73	11.8
	11.85		11.77	
	11.84		11.79	
S-K-2	11.99	12.0	11.89	11.9
	11.97		11.96	
	11.97		11.99	
P-1	10.98	11.0	10.85	10.8
	10.96		10.77	
	10.96		10.75	

#### 4.3.3.2 Hydraulic conductivity

A drilled core sample taken from the test specimens (concrete blocks prepared during the concreting parts of the EPSP construction process) was subjected to testing for permeability measurement purposes. The cylindrical sample (45mm in diameter and 50mm in length) was submitted to an external laboratory (ARCADIS CZ, a. s.) where it was measured according to ČSN CEN ISO/TS 17892-11:2005. A permeability value in the concrete of  $7.9 \cdot 10^{-11} \text{m/s}$  with an uncertainty margin of 2.7% was determined. In addition, a material dry density value of  $2046 \text{kg/m}^3$  was determined for the tested sample.

#### 4.3.4 Laboratory tests on the host rock

Samples of the rock massif were collected from various locations, i.e. from the niche in which the experimental plug was constructed as well as from other parts/niches of the Josef gallery featuring the same type of granitic rock. The drilled core shown in Figure 35 was extracted from borehole V2 which connects the experimental and technical niches of the EPSP project.



Figure 35 - Host rock sample; drilled core from borehole V2

#### 4.3.4.1 Porosity

The drilled core section was cut into smaller samples to be used for the determination of porosity ( $n$ ) using the water submersion method (Melnik and Skeet, 1986). The first stage of testing consisted of the drying of the rock samples and the recording of their weights followed by saturation using synthetic granitic water. Following full saturation, the saturated weights were recorded. The final step of the testing procedure consisted of the evaluation of the surface dry weights of the saturated samples from which sample porosity was calculated. The porosity of the rock samples tested was found to vary according to rock sample composition. Samples of rock "matrices" with no fractures, veins or inhomogeneities were found to exhibit very low porosity values of around 0.15-0.3%, whereas samples with fractures or veins filled with calcite revealed porosity values of up to 1%. The measured data also allowed the calculation of rock density (testing was performed on selected samples only) and, as shown in Tab. 29, the density of rock matrix samples is in the region of 2760-2770kg/m<sup>3</sup>; however, the density of fractured samples was found to be lower.

Tab. 29 - Rock sample porosity and density

rock sample	n (%)	rock density (kg/m <sup>3</sup> )
matrix	0.23	2766
	0.20	2771
	0.19	2765
	0.23	-
	0.17	-
	0.21	-
	0.30	2762
	0.22	2763
	0.28	2762
	0.19	-
	0.15	-
	0.17	-
with filled fractures	0.62	2657
	0.38	-
	0.89	2672
	0.49	-
	0.97	2725

#### 4.3.4.2 Hydraulic conductivity

A sample from a drilled core from the rock matrix was employed for permeability measurement purposes. The sample was submitted to an external laboratory (ARCADIS CZ, a. s.) where it was measured according to ČNS CEN ISO/TS 17892-11:2005. Even when subjected to long-term experimentation, the sample was found to be too impermeable for testing, i.e. it exceeded the limits of the method. Permeability was eventually evaluated as  $< 1 \cdot 10^{-14}$  m/s. A rock density value of 2773kg/m<sup>3</sup> was determined following experimentation involving the test sample.

#### 4.3.5 Physical models

Since the simulation of unsaturated swelling materials is somewhat complicated and the EPSP underground laboratory experiment will not be dismantled during the course of the project, the laboratory work plan proposed the construction of physical models of plugs at the laboratory scale. The aim of these experiments was to collect data for the subsequent calibration of numerical models of the

saturation of the bentonite material. Synthetic granitic water was used in all the experiments and the bentonite material was the same as that used in the EPSP experiment.

Two types of physical model were constructed in the ÚJV's laboratories:

- Physical hydraulic models - PHM
- Physical interaction models - PIM

With regard to the physical hydraulic models (PHM) a sample of compacted bentonite (the same material as that used in EPSP) was fitted with measurement sensors and the sample was gradually saturated. The results of the testing of the physical hydraulic models consisted of curves describing the development of:

- the volume of water which infiltrated into the sample
- the pressure under which the water infiltrated
- the development of RH at 9 observation points
- the development of swelling pressure at the end of the sample

The physical interaction models involved the saturation of the materials (concrete and bentonite) in the same position as in the in-situ EPSP experiment aimed at verifying the anticipated interaction processes between the individual components of the plug. The results of the testing of the physical interaction models consisted of chemical and mineralogical analysis which indicated the potential behaviour of materials in the real EPSP plug (changes in material properties, the formation of new phases, etc.).

The installation of model chambers equipped so as to allow the observation of the progress of water content within the sample was addressed at the beginning of the project prior to the construction of the EPSP proper. Sensors to be employed for the measurement of pore water pressure along with the drainage needles were tested in a small-scale chamber (detail in Figure 36). Samples of bentonite B75 with bulk densities of  $1.2\text{g/cm}^3$  and  $1.6\text{g/cm}^3$  were pressed into small-scale chambers with internal dimensions of 3cm in diameter and 3cm in height and saturated with water under a pressure of 4 bar in the case of the sample with a bulk density of  $1.2\text{g/cm}^3$  and 20 bar in the case of the sample of bulk density  $1.6\text{g/cm}^3$ . The volume of the infiltrating water was measured using a volume meter and the volume of water flowing out of the chamber was monitored using a syringe and drainage needles.



Figure 36 – Detail of drainage needles and sensors for the measurement of pore water pressure

#### 4.3.5.1 Physical hydraulic models

The aim of the PHM was to describe the hydraulic and mechanical processes under way during the saturation of the bentonite. Two PHM models were constructed, one employing bentonite powder and the other bentonite pellets. Two different materials were chosen with respect to subsequent numerical modelling; the repetition of a laboratory experiment using bentonite powder by means of numerical modelling is easier than the simulation of processes under way in bentonite pellets.

Both physical hydraulic models consisted of nine stainless steel chambers of cylindrical shape with dimensions 5cm in length and 8cm in diameter (the total length of the bentonite material in the PHM was 45cm) and were equipped with RH sensors for the recording of the distribution of water content within the bentonite material (Figure 37 and Figure 38). Sensors for the measurement of pore water pressure and the drainage needle were tested in addition to the RH sensor so as to evaluate their use in these types of experiments; however, both pore water pressure sensors and the drainage needle proved to be inadequate for the purpose.

Bentonite with a bulk density of from 1 400kg/m<sup>3</sup> (the same bulk density as that in the EPSP experiment) was pressed into the nine chambers and was gradually saturated with water under pressure. The level of water pressure was determined at 2MPa by means of the field testing of the permeability of the grouted rock in the Josef Underground Laboratory. A sample of the bentonite material was dismantled following the conclusion of experimentation (approximately 1 year - 450 days for the PHM with bentonite powder and 380 days for the PHM with bentonite pellets) and divided into layers with an estimated thickness of 1cm. The water content in each layer was then determined. The data obtained was then added to the data on relative humidity and, together, was compared with the retention curves derived via the block testing method employing small samples.

The following data was recorded during experimentation:

- the volume of water infiltrating into the sample
- the pressure under which the water infiltrated
- the development of RH at 9 observation points
- the development of swelling pressure at the end of the sample

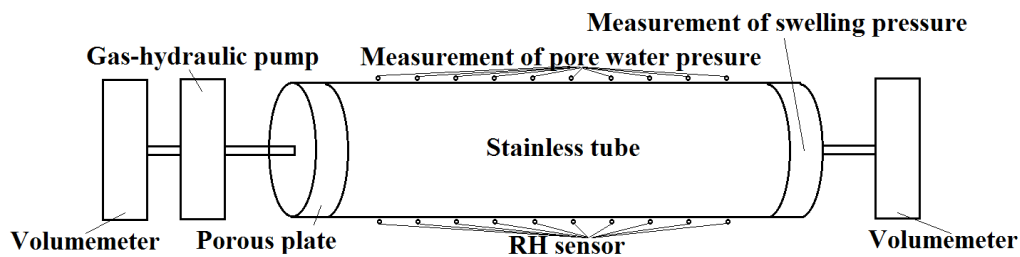


Figure 37 - The geometry of the physical hydraulic model

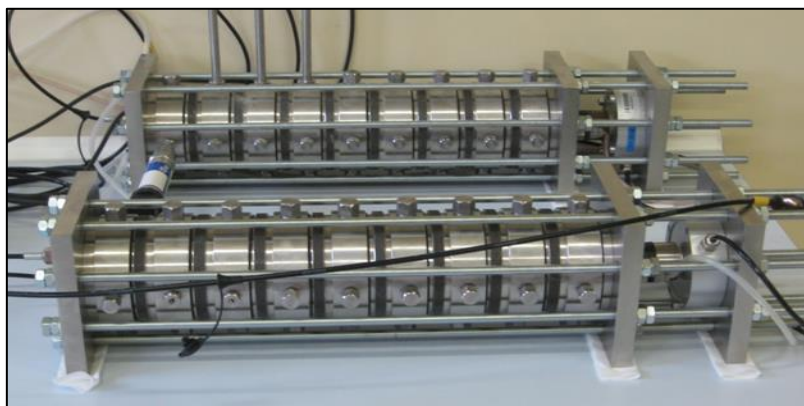


Figure 38 - Physical hydraulic models, one filled with bentonite powder, the second filled with bentonite pellets

#### 4.3.5.1.1 PHM with bentonite powder

The results obtained from the physical hydraulic models with bentonite powder are shown in Figure 39, Figure 40 and Figure 41 which infer that the saturation rate of the material decreases in the direction of flow.

Furthermore, it is apparent that the reaction of swelling pressure is consistent with the reaction of relative humidity at a distance of 2.5cm from the sensor employed for the measurement of swelling pressure (the distance between these two sensors is 2.5cm).

The graphs show that it was possible to maintain constant conditions throughout the duration of the experiment except for a reduction in pressure of 4 bar for a period of around 3 days due to the failure of a reducing valve.

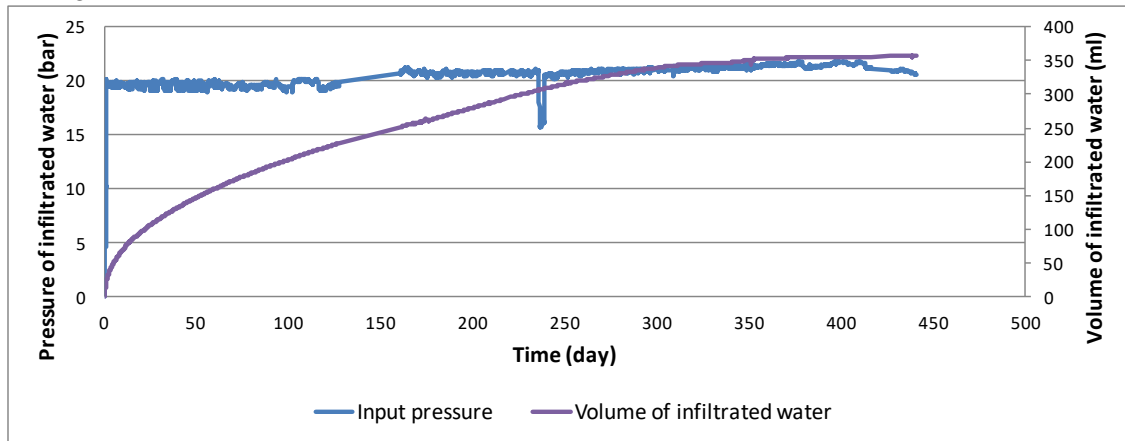


Figure 39 - The pressure and volume of water infiltrating into the sample. The pressure drop on around the 230th day was caused by the failure of a pressure reducing valve

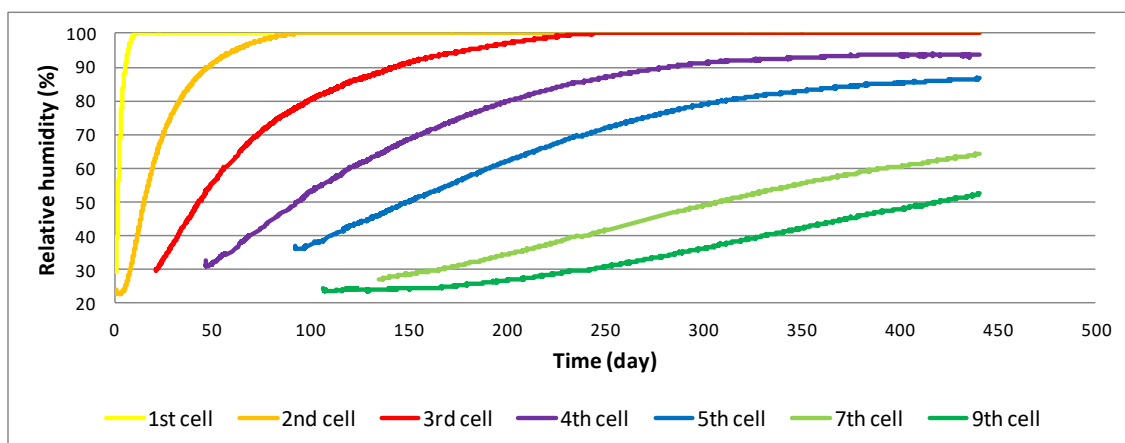


Figure 40 – The development of relative humidity at various observation points

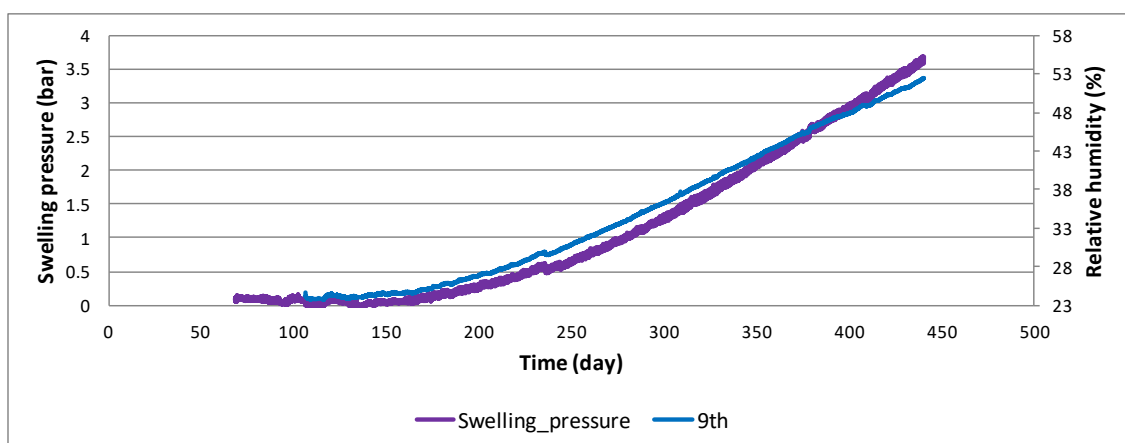


Figure 41 - The development of swelling pressure and relative humidity at the 9th observation point

After a period of around 450 days, the saturation of the bentonite was terminated and the physical model dismantled into individual cells (9 in total, Figure 42). A block of bentonite was extracted from each cell and cut into approximately 1cm thick plates (samples). Subsequently, the water content of each sample was determined; the results are shown in Figure 43.

A comparison of Figure 40 and Figure 43 reveals that although the RH sensors display a value of 100%, the material is not fully saturated. This is due to the principle of the functioning of RH sensors, i.e. such sensors are not capable of measuring a material in a state close to full saturation (Villar, 2007). Figure 43 shows a gradual moisture distribution where the state of the material at the beginning of the physical hydraulic model experiment is controlled by the condition/state of the material at its conclusion.



Figure 42 - The dismantling of the physical hydraulic model into individual cells

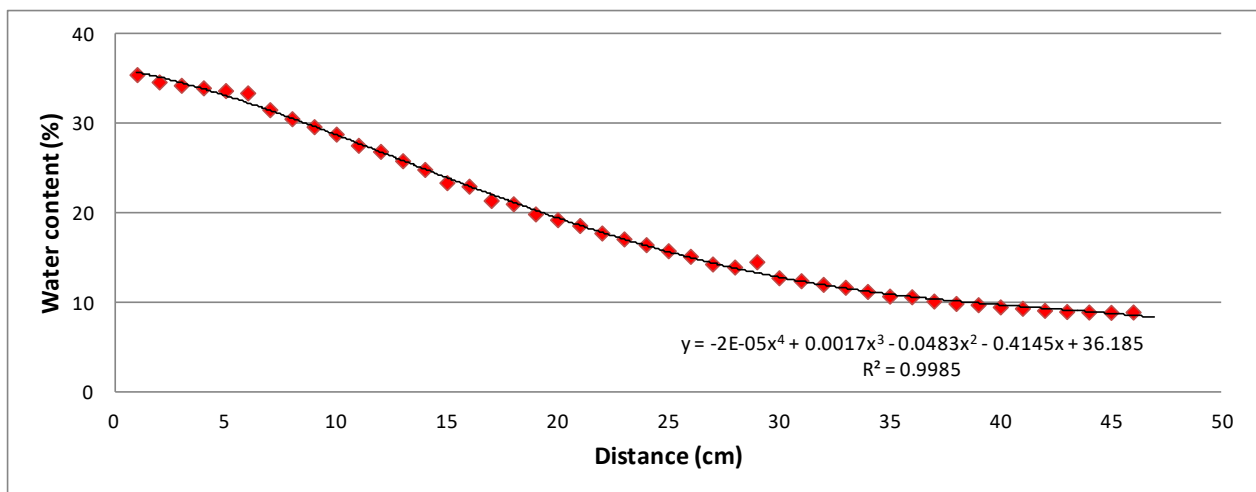


Figure 43 - Profile of mass water content in the PHM, distance indicates the position of the samples from the beginning of the physical model

The moisture retention curve was determined from the measured relative humidity values (after conversion to suction pressure) and the corresponding water content which was compared with the retention curve obtained by using the block method (Figure 44). The results indicate that, despite the difference in scale (the samples used in the block method had a volume of around 53cm<sup>3</sup>), they compare very well.

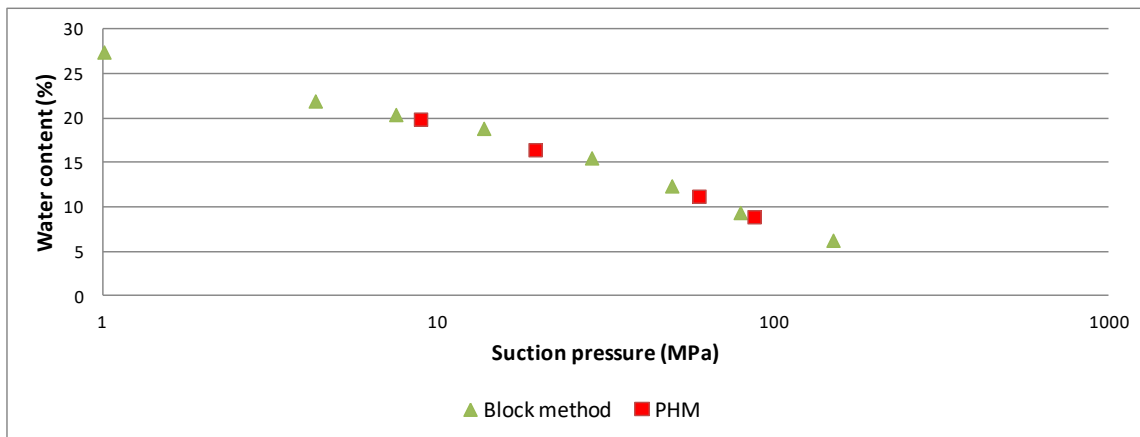


Figure 44 - Comparison of the retention curves of bentonite B75 obtained by the block method and following the dismantling of the physical hydraulic model

#### 4.3.5.1.2 PHM with bentonite pellets

The physical hydraulic model with bentonite pellets had the same geometry as that with bentonite powder. So as to obtain even and continuous saturation, the first cell of the model contained a 5cm thick layer of bentonite powder compacted to a dry bulk density value of  $1400\text{kg/m}^3$  the aim of which was to avoid the suffusion of the void spaces between the pellets by pressurised water and which simulated a layer of low permeability such as concrete; the bentonite pellets were emplaced in the second to ninth cells.

The resulting data is shown in Figure 45, Figure 46 and Figure 47 which reveal the same processes as those acting within the physical hydraulic model with bentonite powder, i.e. the saturation rate of the material decreases in the direction of flow and the reaction of swelling pressure is consistent with the reaction of relative humidity at a distance of 2.5cm from the sensor employed for the measurement of swelling pressure (the distance between these two sensors is 2.5cm).

In contrast to the physical hydraulic model with bentonite powder, the bentonite pellet model was conducted under constant conditions throughout the duration of the experiment; however, during the course of the measurement process the sensor in the fifth cell ceased to function.

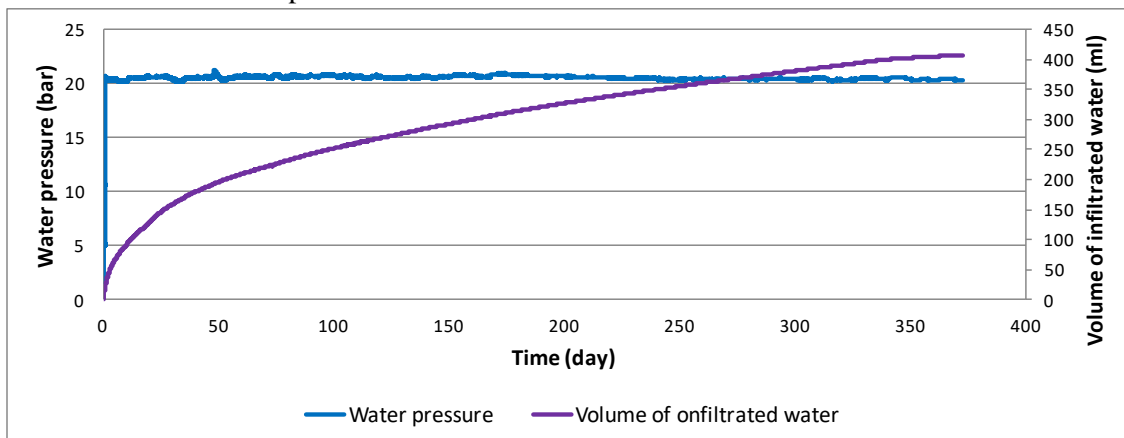


Figure 45 - The pressure and volume of water infiltrating into the sample

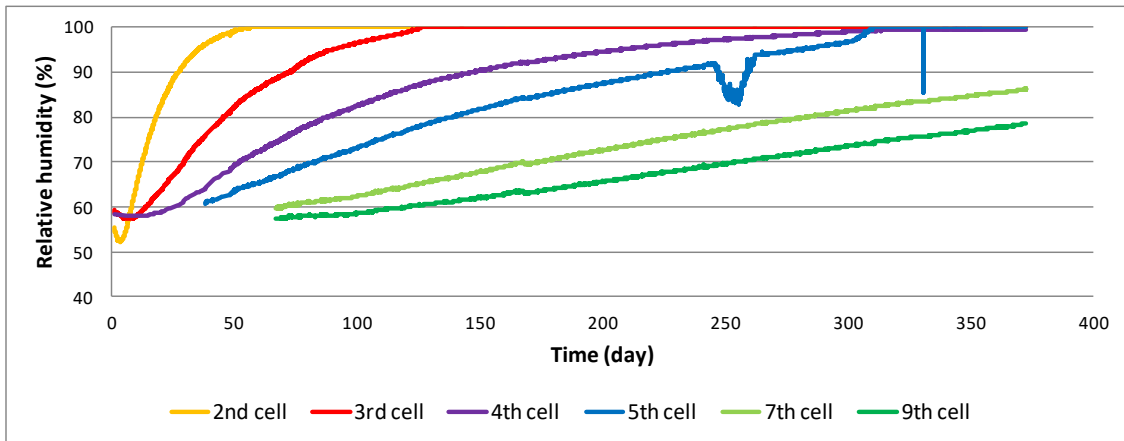


Figure 46 – The development of relative humidity at different observation points. The sensor positioned at the fifth observation point ceased to function during the course of the experiment

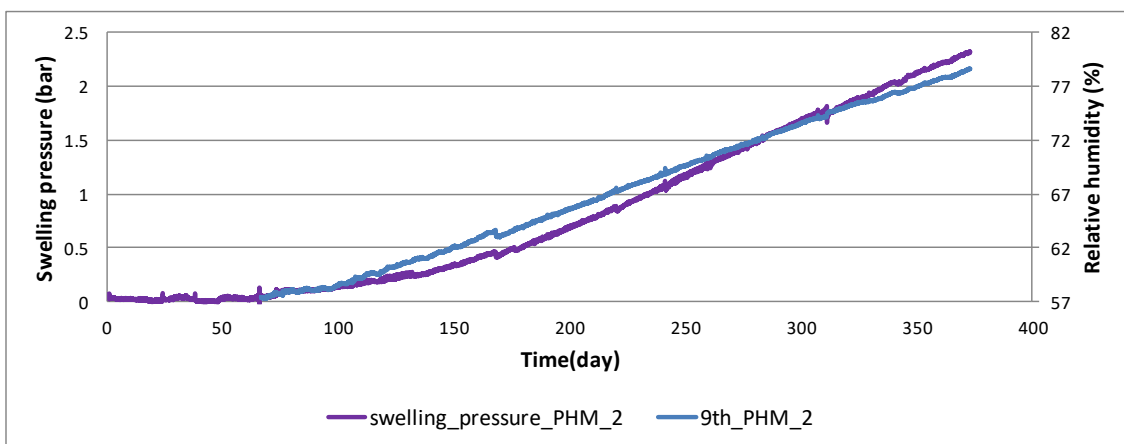


Figure 47 - A comparison of the development of swelling pressure and relative humidity at the 9th observation point

After a period of around 380 days, the saturation of the bentonite was terminated and the physical model dismantled into individual cells (9 in total). A block of bentonite was extracted from each cell and cut into approximately 1cm thick plates (samples). Subsequently, the water content of each sample was determined; the results are shown in Figure 48.

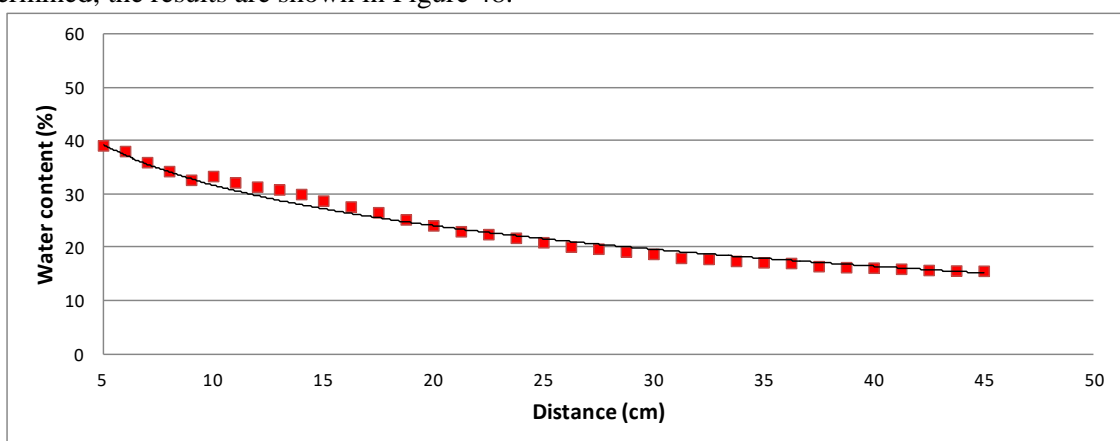


Figure 48 - Profile of mass water content in the PHM with bentonite pellets, distance indicates the position of the samples from the beginning of the physical model

#### 4.3.5.2 Physical interaction models

A physical interaction model (PIM) for the study of the interaction of various materials used in the experimental plug was designed, and experimentation commenced, in 2014. Exactly the same materials were used as those in the experimental plug. Synthetic granitic water was used as the liquid phase for the study of saturation and interaction processes. The PIM consisted of three stainless steel cylinders with a diameter of 8cm and a length of 5cm each; the total length of the model was 15cm. This arrangement was decided in an effort to best approximate the geometry of the real in-situ EPSP plug. Bentonite powder was pressed into the middle part so as to reach a dry density value of  $1400\text{kg/m}^3$ ; this part was then surrounded by two cylindrical blocks of low-pH concrete. The geometry of the physical interaction model is shown in Figure 49. The concrete blocks were prepared from a drill core which was sampled following the testing of shotcreting technology in the Josef gallery. Polyurethane grouting materials and a silicone sealant were used for the sealing of the concrete blocks in a steel cell so as to ensure the passage of water through the concrete sample only. A synthetic granitic water source under a pressure of 2MPa was connected to one side of the PIM. The input water pressure was continuously recorded by means of a data logger. So as to avoid damage to the relative humidity sensor, it was removed from the experimental cell during the experiment once the bentonite layer had become saturated.

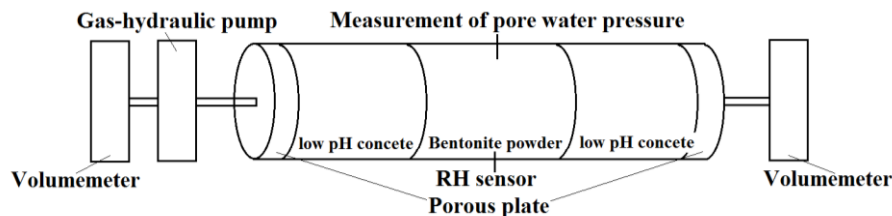


Figure 49 - The geometry of the physical interaction model

The quantity of outflowing water was continuously monitored following the attainment of the steady state (see Figure 50) and the water was sampled for chemical analyses. Initial analysis revealed significant changes in the composition of the aqueous phase. The outflowing water from the PIM exhibited significant enrichment in all major cations and anions in comparison to input synthetic granitic water. A similar degree and content of enrichment was also observed following an analysis of the aqueous phase sampled in the output of the bentonite hydraulic permeability tests.

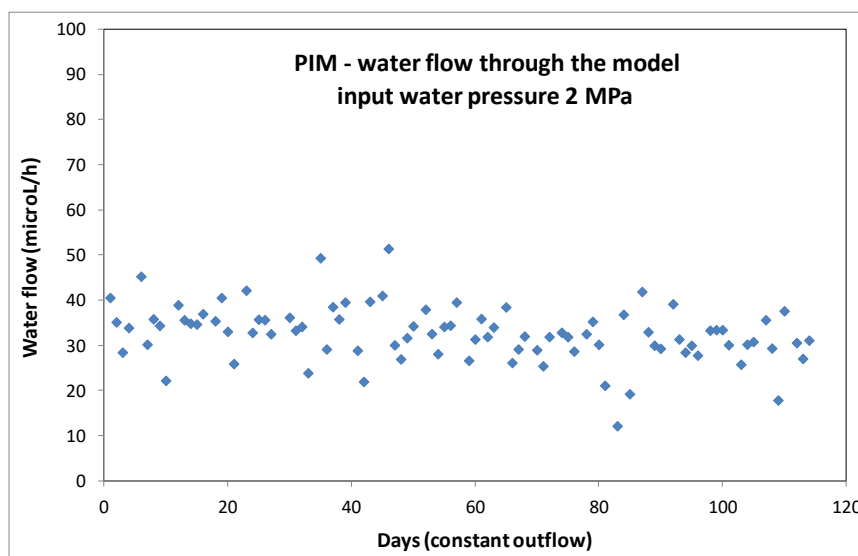


Figure 50 - Steady state water flow through the interaction model; input water pressure 2MPa

Following the dismantling of the PIM, all the materials were studied for the determination of interaction products and so as to compare the physical and chemical properties of the materials prior to and following the termination of the experiment (i.e. mineralogy, porosity, CEC, pH of the leachate, chemical composition, etc.). In addition, during the dismantling phase (Figure 51) all the materials were sampled for analysis and measurement purposes. During the dismantling phase of the model, the bentonite block was divided into 6 different slices (Figure 52) in the direction from the water output to the input – one slice of swelled bentonite material (denoted as 2mm) and five slices (denoted as A to E), each approx. 1 cm thick. Each slice A to E was then divided into five parts (denoted as 1 to 5, see Figure 53) for the water content analysis according to ISO/TS 17892-1.



Figure 51 - Dismantling of the PIM

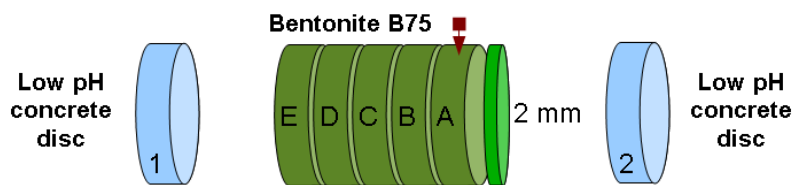


Figure 52 - Dismantling of the PIM – bentonite slices

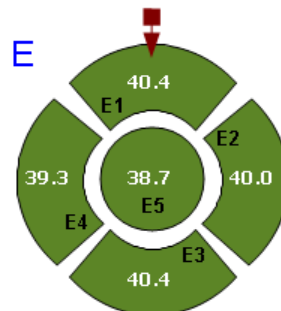


Figure 53 - Example of a bentonite slice divided to parts for water content determination, with determined water content values (wt%)

#### 4.3.5.2.1 Water content analysis of dismantled PIM

During the dismantling phase of the model, following parts were analyzed for its water content: both low pH concrete discs, grouting from both sides of the model and bentonite block. Concrete discs and grouting were analyzed in the state they were removed from the steel cells; bentonite block was divided in 6 slices – one 2mm thick (swelled bentonite out from the steel ring of the cell at the bentonite interface with output concrete disc) and five approx. 1 cm thick (denoted as A to E in the direction from output concrete disc to input in Figure 52). All slices A to E were then divided into five parts denoted as 1 to 5

in Figure 53 (red arrow indicates the position of the first part of each slice relative to the steel ring orientation). Then the water content according to ISO/TS 17892-1 was determined in all bentonite samples and concrete discs. In the following table (Tab. 30), water content is listed in the order from the output to the input of PIM. As can be seen from this table, the water content of bentonite block decreases in the direction to the output concrete disc that has also lower water content than the input concrete disc (11.7 wt% vs.14.8 wt%). From the section analysis of each slice (except the 2mm slice) there are no significant differences among water content depending on the position of the bentonite sample, except the slice E. In this slice, the water content of bentonite in the central part (5E) is lower in comparison to its periphery, which suggests the water inflow to the bentonite through the grouted concrete/steel ring interface rather than through the whole part of the concrete disc.

*Tab. 30 – Water content in parts of PIM*

<b>Sample</b>	<b>Water content (wt%)</b>
Output concrete (2)	11.7
2mm	35.9
1A	36.9
2A	37.1
3A	36.6
4A	36.5
5A	36.1
1B	36.1
2B	37.0
3B	36.5
4B	36.6
5B	36.5
1C	37.3
2C	37.5
3C	37.3
4C	37.0
5C	38.2
1D	39.1
2D	38.6
3D	38.7
4D	38.8
5D	39.1
1E	40.4
2E	40.0
3E	40.4
4E	39.3
5E	38.7
Input concrete (1)	14.8

This assumption was confirmed by the water content analysis of grouting material used to seal the concrete/steel interface in the PIM. For the input concrete sample, water content in grouting was found to be distributed unevenly, 16.6 wt% in one part and 20.5 wt% in the second part. On the other hand, grouting used in the output part of the PIM had the water content only 7.4 wt% and 8.9 wt% in two parts.

According to water content analysis it can be concluded that bentonite block simulating the bentonite sealing part of the plug is saturated in the case of PIM incompletely. The part close to the input concrete disc has generally higher water content, especially in the zone in contact with the steel ring of the supporting ring that could be caused by the stronger saturation through the grouting used to seal the concrete/steel interface.

#### 4.3.5.2.2 Trends in chemical composition of water sampled from PIM

For PIM saturation, the synthetic granitic groundwater (SGW) with composition listed in Tab. 2 was used. The SGW was taken from the reservoir and pumped to the PIM under the constant pressure 2 MPa using gas-hydraulic pump. First sample collected at the output of PIM was taken more than 4 months after the start of the PIM experiment. In comparison to SGW, this PIM water was significantly enriched in all analyzed ions with exception of nitrates and fluorides (Tab. 31). Because of very low amount of water collected, the analysis of bicarbonate ions wasn't performed and its content was calculated – more than 7.6g/l of bicarbonate is needed to ensure ionic balance. Because of potentiometric determination of bicarbonates requires large amount of liquid sample and the flow through the PIM was very low, required sample was collected in closed system approximately two months after the first sampling. In this sample, bicarbonate amount was determined to be approx. 4.3g/l at pH 7.6. When the constant flow through the PIM was achieved, the amount of outflowing water was monitored and samples collected for chemical analyses. In all samples, total concentrations of Na, K, Mg and Ca were analyzed using atomic absorption spectroscopy technique, concentrations of anionic species (sulphates, chlorides, nitrates) were analyzed using ionic chromatography technique and concentrations of bicarbonates were determined using potentiometric titration. The pH of samples varied in the range 7.1-7.7 and the conductivity of water decreased from 8.7mS/cm (for the first sample) to 5.8mS/cm (for the last sample). The evolution of major cations and anions concentrations in PIM water samples with the time (and the amount of flowing water) are presented in Figure 54, Figure 55 and Figure 56. The concentration of bicarbonates changed from 3.1 g/l in the first sampling point of constant outflow to 1.8g/l in the last sampling point before the PIM dismantling. Analyzes of water samples from the PIM were compared to analyzes of water samples from hydraulic conductivity tests performed for bentonite pellets compacted to 1400kg/m<sup>3</sup> in large cells (denoted as PROPs). It was found that PIM water samples are significantly enriched in calcium and potassium in comparison to water samples obtained from PROPs (see Figure 57).

Tab. 31 – Comparison of SGW composition to PIM water composition

	<b>SGW (mg/l)</b>	<b>PIM water (1<sup>st</sup> sample) (mg/l)</b>
Na	10.6	1649
K	1.8	268
Mg	6.4	151
Ca	27.0	1695
Cl	42.4	426
SO <sub>4</sub>	27.7	1845
NO <sub>3</sub>	6.3	0.1
F	0.2	N.D.
HCO <sub>3</sub>	30.4	N.A.

Note: N.D. - not detected, N.A. - not analyzed

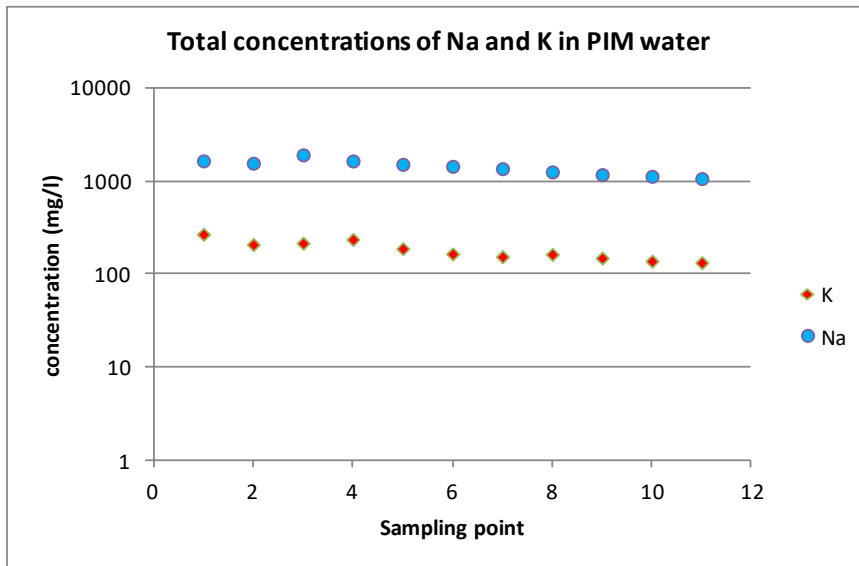


Figure 54 – Evolution of total concentrations of sodium and potassium in PIM water with time. Constant water outflow observed after the 4<sup>th</sup> sampling point. Time interval between the first and the 4<sup>th</sup> sampling point is approx. 3 months, between the 4<sup>th</sup> and the last sampling point is approx 4 months.

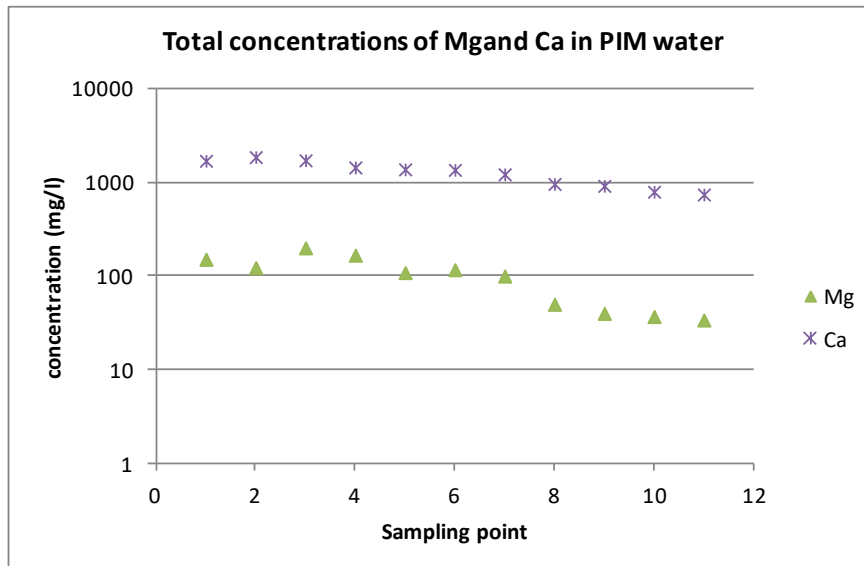


Figure 55 – Evolution of total concentrations of magnesium and calcium in PIM water with time. Constant water outflow observed after the 4<sup>th</sup> sampling point. Time interval between the first and the 4<sup>th</sup> sampling point is approx. 3 months, between the 4<sup>th</sup> and the last sampling point is approx 4 months.

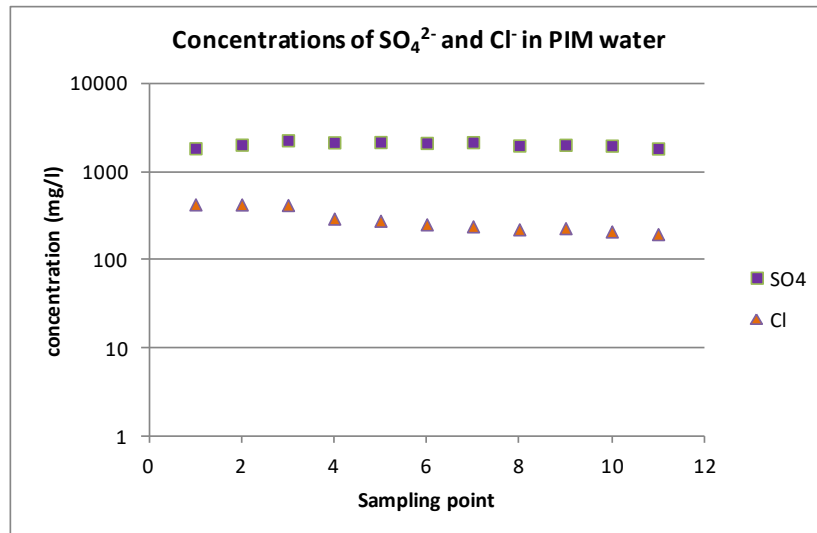


Figure 56 – Evolution of concentrations of sulphates and chlorides in PIM water with time. Constant water outflow observed after the 4<sup>th</sup> sampling point. Time interval between the first and the 4<sup>th</sup> sampling point is approx. 3 months, between the 4<sup>th</sup> and the last sampling point is approx 4 months.

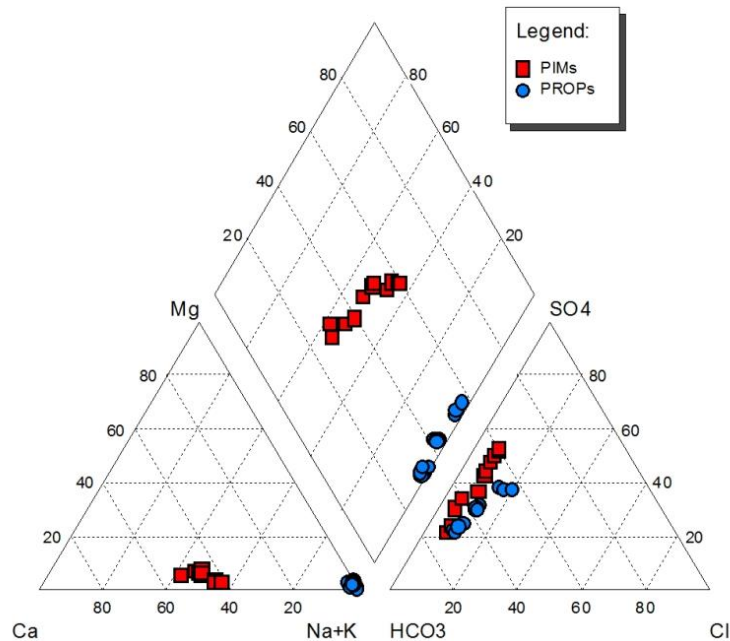


Figure 57– Piper diagram of PIM and PROP water samples

The analysis of analytical data and their equilibrium calculations in PHREEQC geochemical code showed oversaturation with respect to the carbonate minerals (calcite, dolomite) and also gypsum. In addition to oversaturated phases, significant amount of non-ionic species in solutions was calculated at equilibrium, especially  $\text{CaSO}_4^0$  and  $\text{MgSO}_4^0$  in PIM samples. As oversaturation with respect to the carbonate minerals was calculated in all PIM water samples, it was expected that these minerals would be present in PIM material interfaces (concrete/bentonite) because of concrete acts as calcium source and bentonite as carbonate source due to activation reagent presence. During the PIM dismantling, samples of visually different spots present at the bentonite part of both input and output interface were taken and mineralogical analyzes were performed. With comparison to input bentonite material (B75 pellet), only in one sample the relative increase of calcite was detected.

#### 4.3.5.2.3 Cation exchange capacity of selected bentonite samples

After the PIM dismantling, samples of bentonite taken from selected slices and its parts were analyzed for their cation exchange capacity (CEC) and exchangeable cations. Complete slice 2mm, all five parts of the E slice and two central parts (slice A and C) were analyzed using Cu-triethylenetetramine method (Meier and Kahr, 1999). As can be seen from Tab. 32, total CEC of all selected samples is practical unchanged in comparison with B75 pellet sample, with respect to the analytical determination uncertainties. But as can be seen from Tab. 33, the exchangeable cations from the B75 pellet sample are significantly different in comparison to PIM samples – changing from Mg-Na to Ca-Mg occupancy of exchangeable sites.

Tab. 32 – CEC of selected PIM bentonite samples

Sample	CEC (meq/100g)
2mm	55.1
5A	56.6
5C	57.3
1E	57.0
2E	54.9
3E	55.6
4E	56.9
5E	58.0
B75 pellet	56.4

Tab. 33 – PIM bentonite samples ionic form

Sample	Na (meq/100g)	K (meq/100g)	Mg (meq/100g)	Ca (meq/100g)
2mm	13	4	19	29
5A	15	4	20	31
5C	14	5	22	28
1E	14	5	22	29
2E	13	5	21	27
3E	13	5	21	28
4E	14	5	22	27
5E	15	5	21	29
B75 pellet	18	4	31	10

It can be concluded that the concrete part of the PIM acts as calcium source that is exchanged for sodium and magnesium in bentonite. As can be seen from Tab. 33, more magnesium than sodium is exchanged for calcium in bentonite ion exchange complex and this magnesium is then released to outflowing water (compare input SGW composition in Tab. 31 with PIM water and Figure 55). According to the water content results and CEC analysis it can be said that the bentonite of the PIM was homogeneously saturated by the calcium-enriched water from the input concrete disc of the PIM. High sodium concentrations in outflowing water (Figure 54) are probably caused predominantly by the leaching of unknown amount of activation reagent residues (sodium carbonate) in bentonite B75 rather than by ion exchange process. Similar high sodium concentrations in outflowing waters from hydraulic conductivity tests (PROPs) were found which supports this explanation (also compare with Tab. 24 and high sodium amount in water leachates of bentonite B75). Also potassium released from concrete part is suppressed by divalent calcium during the exchange and is released to outflowing water (exchangeable potassium remains the same).

#### 4.3.5.2.4 Specific surface area of selected bentonite samples

Bentonite samples selected for the CEC analysis (complete slice 2mm, all five parts of the E slice and two central parts (slice A and C)) were also analyzed for their specific surface area (SSA) using EGME method (Carter et al., 1986). The main aim of this analysis was to compare SSA of the input bentonite (B75\_2013 in the form of pellet) with SSA of bentonite from various parts of the PIM. Because of EGME method provides the value of total specific surface area for expanding clay minerals (sum of external and internal surface), it can point to mineralogical changes in these minerals caused by the alteration processes that results in changes of expandability (internal surface of these minerals is much more higher than external). Because of higher amount of bentonite in comparison to concrete material in PIM (and its lower reaction surface in contact with bentonite) and short contact time (with respect to possible mineralogical changes), significant alterations were not expected. As can be seen from Tab. 34, although some minor difference in specific surface area among PIM bentonite samples, generally their values of SSA are close to the value of the source bentonite B75. Slightly higher values of SAA of PIM bentonite samples are probably connected with exchangeable complex. The divalent cations in exchangeable complex, such as Mg and Ca can increases the SSA value.

Tab. 34 – Specific surface of selected PIM bentonite samples

Sample	specific surface area (m <sup>2</sup> /g)
2mm	430 ± 28
5A	491 ± 17
5C	476 ± 18
1E	482 ± 36
2E	466 ± 7
3E	465 ± 7
4E	478 ± 11
5E	491 ± 8
B75 pellet	453 ± 18

#### 4.3.5.3 Concrete after PIM dismantling

##### *Leachate pH*

The methodology of SKB report R-12-02 (Alonso et al., 2012) for pH measurement in cement leachate was applied. It wasn't observed any significant change in the pH of the leachate of concrete material obtained from PIM dismantling. The pH value varied about 11.5 with the respect to experimental error. It could be concluded that from this point of view there was no change in the concrete leachate pH after the interaction with bentonite and synthetic granitic water.

##### *Porosity*

For porosity studies two method were used, to evaluate the porosity of concrete after dismantling Physical Interaction Model, the mercury intrusion porosimetry and water submersion method (Melynk and Skeet, 1986). For each method, own samples were used, so it is not possible to compare the results on the exactly same sample. Limits of the apparatus for mercury porosimetry require small samples at maximal dimensions 8×8×35 mm. For water submersion method samples in cm scale are used (see Figure 58). Both method have limitations, too small samples for mercury porosimetry are not representative for whole block of concrete same as the ratio of aggregates and concrete, water submersion method, originally developed for igneous rock samples, are not very suitable for samples with higher porosities such as concrete.

Mercury porosimetry was performed in external laboratory and obtained values vary in range 14.6 - 19.3%, probably due to inhomogeneity of small samples. Water submersion method was performed in

ÚJV laboratories and obtained results are higher, in comparison to mercury porosimetry, 20.4 - 23.6%. The variance in results is caused by differences in used techniques. Values of porosity obtained for samples from dismantled PIM and samples of concrete nor interacted with bentonite and SGW are comparable with respect to experimental and methodology errors, 20 - 25%.

The porosity of concrete was not affected by interaction with bentonite and synthetic granitic water during the run of the interaction model



Figure 58- Concrete samples for porosity measurements, on left - samples for mercury intrusion porosimetry, on right - samples for water submersion method

#### 4.3.6 Conclusion of the ÚJV's work

The goal of the work of the ÚJV laboratories focused principally on general material characterisation and testing, the characterisation of selected types of materials, the confirmation of the properties of the input materials used for EPSP construction and the study of changes in materials and their interactions during experiments.

The host rock was characterised based on drill core samples in terms of porosity and permeability. It was discovered that even though the rock massif in the Josef gallery is somewhat fractured and disturbed, the undisturbed parts exhibit very low levels of permeability and porosity.

It was also determined that common polyurethane-based grouting materials are not influenced by alkaline solutions and should not be affected by cement leachates originating in the grouting of the experimental plug. In addition, the polyurethane material itself was found not to leak during permeability testing under a pressure of 2.5MPa.

With regard to the various cement/concrete materials, ÚJV testing focused primarily on the measurement of pH. It was verified that increasing the SiO<sub>2</sub> content in the mixture (ratio of cement/SiO<sub>2</sub> = 1/1) leads to a decrease in the pH value of the leachate in distilled water (according to a procedure based on Alonso et al. (2012)) to a pH value of ~ 11.5. The pH value of the leachate from the concrete used in the construction of the experimental plug fulfils the limits verified by means of laboratory tests on samples obtained from both the inner and outer concrete parts of the EPSP (pH = 11.4-11.5).

The properties of bentonite materials were studied in order to confirm the selection of the most suitable material. The analysis of chemical composition and mineralogy, the measurement of pH in bentonite suspensions and distilled water with different ratios, the analysis of leachates and the measurement of porosity were conducted with regard to B75\_2013 bentonite which was selected as the construction material for the EPSP. Further, it was confirmed that the main characteristics of B75 bentonite fulfil all the various expectations, limits and requirements for the EPSP seal.

In addition, the equipment (cells, sensors etc.) destined for use in the laboratory physical models was successfully tested and installed in the various experimental models. The results of tests on the laboratory physical models (using the same materials as those employed in the construction of the experimental plug in situ) were used as input material for mathematical modelling in WP5.

## 5 CONCLUSION

The laboratory research was undertaken as a supporting activity for the construction of the EPSP experiment. One of the main aims of EPSP is the use of Czech materials and available technologies. Factory-produced Czech bentonite (milled, non-activated Ca-Mg type) was selected as the principal material for the sealing part of the plug (the commercial product “Bentonit 75”). Various laboratory tests were performed on B75\_2013 (batch from 2013) material to verify its properties. Laboratory tests focused also on cement/ concrete, grouting substances and rock samples parameters.

Basic laboratory tests by CTU were aimed at the of key geotechnical parameters of both the bentonite powder and compacted samples. The testing of the most appropriate technology for the manufacture of the pellets, in cooperation with potential Czech producers, was then carried out. After verification of sealing properties of pellets the main conclusion was that B75\_2013 bentonite pellets demonstrated sufficient dry density levels and corresponding sealing properties and therefore they can be used to achieve the required geotechnical behaviour of the bentonite seal in the EPSP experiment.

It was planned that a bentonite-ice mixture would be used for the DOPAS sealing section. Therefore, several tests were performed in order to verify the feasibility of its use with respect to the technology available and the specific requirements of the EPSP experiment (the total amount of material required, capacity per hour, distance from the ice source etc.). Based on the results of these tests and on the very limited time available for bentonite application, the use of ice was ruled out. Compaction employing ordinary plates and spraying technology was chosen for final application. In-situ sampling was conducted during the construction of the EPSP bentonite sealing section so as to monitor the achieved dry density of the pellet layer. Requirement pertaining to dry density ( $1.4\text{Mg/m}^3$ ) was fulfilled with regard to the whole volume of the seal.

Responsibility for the verification testing of concrete quality during and after construction was accorded to CTU subcontractor Metrostav a. s. During negotiations on the initial contract, some changes in testing plan were agreed to provide for the improved monitoring of both fresh and hardened concrete. It can be concluded that all the parameters tested by CTU/ Metrostav a. s. fulfilled the required criteria.

Responsibility for the verification testing of improvement of rock massif around the EPSP experiment was accorded to SÚRAO subcontractor Arcadis a. s. The rock massif was improved by means of grouting using polyurethane resins. Significantly lower values of permeability were confirmed by the results of water pressure testing after grouting. Other measurements taken of the various geotechnical parameters concerned the overall conditions of the rock mass.

The goal of the work of the ÚJV laboratories focused principally on general material characterisation and testing, the characterisation of selected types of materials (bentonite, concrete, grouting materials). Laboratory test on bentonite performed by ÚJV mainly focused on its chemical composition, the measurement of pH in suspensions of bentonite and distilled water at different ratios and the analysis of leachates (cation concentrations). With regard to the various cement/concrete materials, ÚJV testing focused primarily on the measurement of pH. The host rock was characterised based on drill core samples in terms of porosity and permeability. It was concluded that the main characteristics of B75 bentonite remained constant and other materials (cement/ concrete, grouting substances, grouted rock) fulfilled all the expectations, limits and requirements for the construction of the experimental plug.

Two laboratory tests using physical models were conducted by ÚJV. The overall objective of these experiments is to derive data for the subsequent calibration of numerical models of the saturation of the bentonite material, and to study the interactions between the bentonite and grouted granite, and between the concrete and grouted granite interfaces. The results of tests on the laboratory physical models (using the same materials as those employed in the construction of the experimental plug in situ) were used as input material for mathematical modelling in WP5.

## 6 REFERENCES

- Alonso M. C., García Calvo J. L., Walker C., Naito M., Pettersson S., Puigdomenech I., Cuñado M. A., Vuorio M. Weber H., Ueda H., Fujisaki K.: SKB report R-12-02. Development of an accurate pH measurement methodology for the pore fluids of low pH cementitious materials. SKB, Stockholm, Sweden, 2012.
- Applied Precision. ISOMET 2114 user manual. Applied Precision. Bratislava, 2014
- Applied Precision. "ISOMET." Applied Precision Ltd. Web. 18 Dec. 2015. <<http://www.appliedp.com/en/isomet.htm>>.
- Malý, V. EXPERIMENT EPSP – DOPAS; As-built Documentation: Grouting, drilling and sealing operations for the EPSP experiment conducted under the DOPAS international project, SÚRAO contract no. SO2013-073, Arcadis, a. s., March 2015, Prague
- Carter D.L., Mortland M.M., Kemper W.D. Specific surface, In: Klutke A. Ed. Methods of Soil Analysis, Part I. Physical and Mineralogical Methods – Agronomy Monograph no. 9 (2<sup>nd</sup> Edition), Madison, Wisconsin, pp 413-423. 1986
- Červinka R., Hanuláková D. Laboratorní výzkum tlumících, výplňových a konstrukčních materiálů. Geochemické modelování bentonitová pórová voda. Report ÚJV Rež, a. s., 14269, May 2013, 111 p. in Czech
- Červinka R., Vejsadů J., Vokál A. Uncertainties in the pore water chemistry of compacted bentonite from the Rokle deposit, Clays in natural and engineered barriers for radioactive waste confinement, 5th International Meeting, 21.-25.10.2012, Montpellier, France, P/GC/T/6, p. 467-468.
- ČSN CEN ISO/TS 17892-1 Geotechnical investigation and testing - Laboratory testing of soil - Part 1: Determination of water content. ICS 13.080.20; 93.020. Ed. 1, Prague, Czech Office for Standards, Metrology and Testing, May 2005.
- ČSN EN ISO 17892-2:2014 Geotechnical investigation and testing - Laboratory testing of soil - Part 2: Determination of bulk density. ICS 13.080.20; 93.020. Ed. 1, Prague, Czech Office for Standards, Metrology and Testing, May 2015.
- ČSN CEN ISO/TS 17892-3 Geotechnical investigation and testing - Laboratory testing of soil - Part 3: Determination of particle density - Pycnometer method. ICS 13.080.20; 93.020. Ed. 1, Prague, Czech Office for Standards, Metrology and Testing, May 2005.
- ČSN CEN ISO/TS 17892-11 Geotechnical investigation and testing - Laboratory testing of soil - Part 11: Determination of permeability by constant and falling head. ICS 13.080.20; 93.020. Ed. 1, Prague, Czech Office for Standards, Metrology and Testing, May 2005.
- ČSN CEN ISO/TS 17892-12 Geotechnical investigation and testing - Laboratory testing of soil - Part 12: Determination of Atterberg limits. ICS 13.080.20; 93.020. Ed. 1, Prague, Czech Office for Standards, Metrology and Testing, May 2005.
- ČSN EN 1926 Natural stone test methods - Determination of uniaxial compressive strength. ICS 73.020; 91.100.15. Ed. 2, Prague, Czech Office for Standards, Metrology and Testing, July 2007
- ČSN EN 1997-2 Eurocode 7: Geotechnical design - Part 2: Ground investigation and testing. ICS 91.060.01; 91.120.20. Ed. 1, Prague, Czech Office for Standards, Metrology and Testing, April 2008
- ČSN EN 12350-5 Testing fresh concrete. Flow table test. ICS 91.1200.30. Ed. 2, Prague, Czech Office for Standards, Metrology and Testing, October 2009.
- ČSN EN 12390-3/Z1 Testing hardened concrete. Compressive strength of test specimens. ICS: 91.100.30. Ed. 1 – rev. 1, Prague, Czech Office for Standards, Metrology and Testing, November 2012.
- ČSN EN 12390-7 Testing hardened concrete. Density of hardened concrete. ICS 91.100.30. Ed. 1, Prague, Czech Office for Standards, Metrology and Testing, November 2009.

- ČSN EN 12504-1 Testing concrete in structures. Cored specimens. Taking, examining and testing in compression. ICS 91.100.30. Ed. 2, Prague, Czech Office for Standards, Metrology and Testing, November 2009.
- ČSN EN 14488-3 Testing sprayed concrete. Flexural strengths (first peak, ultimate and residual) of fibre reinforced beam specimens. ICS 91.100.30. Ed. 1, Prague, Czech Office for Standards, Metrology and Testing, December 2006.
- ČSN ISO 6784 (731319) - Concrete. Determination of the static modulus of elasticity in compression. MDT 691.32:620.173.22. Ed. 1, Prague, Czech Office for Standards, Metrology and Testing, May 2005.
- Dixon, D. A., Graham, J. and Gray, M. N. Hydraulic conductivity of clays in confined tests under low hydraulic gradients. *Can. Geotech. J.* 1999, vol. 36, no. 5, s. 815-825. DOI: 0008-3674. Available at: <http://hdl.handle.net/1993/2792>
- Dixon, D., Sandén, T., Jonsson, E., Hansen, J., SKB report P-11-44: Backfilling of deposition tunnels: Use of bentonite pellets, February 2011
- Filala, Z., Sosna, K., Šebelová, J. & Záruba, J. (2014). Laboratorní stanovení modulů pružnosti a přetvárnosti, pevnosti v prostém tlaku a pevnosti v příčném tahu, Arcadis CZ a.s. Archív SÚRAO (in Czech).
- Franče J. Bentonity ve východní části Doupovských hor. Sborník geologických věd, Ložisková geologie a mineralogie 30, 43-90. 1992.
- Havlová V., Holeček J., Vejsada J., Večerník P., Červinka R. Metodika přípravy syntetické podzemní vody pro laboratorní experimentální práce. Technical report of the FR-TI1/367 project, February 2010, 11 p., in Czech
- Hoffmann, C., Alonso, E., Romero, E. 2007. Hydro-mechanical behaviour of bentonite pellet mixtures. *Physics and Chemistry of the Earth, Parts A/B/C* [online]., 32(8-14): 832-849 [cit. 2015-09-30]. DOI:10.1016/j.pce.2006.04.037. ISSN 14747065. Available at: <http://linkinghub.elsevier.com/retrieve/pii/S1474706506002415>
- Karnland, O., Nilsson, U., Weber, H., Wersin, P. Sealing ability of Wyoming bentonite pellets foreseen as buffer material – Laboratory results, *Physics and Chemistry of the Earth, Parts A/B/C, Volume 33, Supplement 1, 2008, Pages S472-S475, ISSN 1474-7065, (http://www.sciencedirect.com/science/article/pii/S1474706508003070)*
- Meier L.P., Kahr G. Determination of the cation exchange capacity (CEC) of clay minerals using the complexes of copper(II) ion with triethylenetetramine and tetraethylenepentamine, *Clays and Clay Minerals* 47, pp 386-388. 1999
- Melnyk T.W., Skeet A.M.M. An improved technique for the determination of rock porosity. *Can. J. Earth Sc.* Vol 23, pp 1068-1074. 1986
- Myšičková, L., Protokol o provedení zkoušky rozliti – zátka č. 2 – vnitřní; podle ČSN EN 12350-5. Metrostav a. s., Prague, November 2014
- Myšičková, L., Protokol o provedení zkoušky rozliti – zátka č. 1 – vnější; podle ČSN EN 12350-5. Metrostav a. s., Prague, June 2015
- Petružálek, M., Nemejovský, V. Stanovení koeficientu filtrace betonových vzorků – závěrečná zpráva. Institut of Geology of the Czech Academy of Science. Prague, January 2015
- Slanina, M. (a) Protokol o zkoušce pevnosti betonu v tlaku podle ČSN EN 12504-1 (Vývrty), no. B/438/14; SQZ s.r.o., Prague 5, 12 December 2014
- Slanina, M. (b). Protokol o zkoušce stříkaného betonu podle ČSN EN 14488-3, no. B/439/14; SQZ s.r.o., Prague 5, 12 December 2014
- Slanina, M. (a) Protokol o zkoušce pevnosti betonu v tlaku, no. B/310/15; SQZ s.r.o., Prague 5, 17 July 2015
- Slanina, M. (b). Protokol o zkoušce stanovení ohybové únosnosti vláknobetonu, no. B/311/15; SQZ s.r.o., Prague 5, 17 July 2015

- Sosna, K., Černý, D., Kvarda, M., Tocháček, M. & Záruba, J. (a). Stanovení deformačních modulů in situ pomocí zkoušky Goodman Jack, Arcadis CZ a.s. Archív SÚRAO (in Czech), 2014
- Sosna, K., Vysoká, H. & Záruba, J. (b). Výsledky vodních tlakových zkoušek ve vrtu VTZ-4, 5, 6 a VTZM-2, 3, 4, Arcadis CZ a.s. (in Czech). 2014.
- Svoboda, J., Vašíček, R., Smutek, J., Šťáštka, J. *Deliverable D3.15 Detail design of EPSP plug*. DOPAS project FP7 EURATOM, no. 323273; Czech Technical University in Prague, Prague, 28 February 2015
- Svoboda, J., Vašíček, R., Smutek, J., Šťáštka, J. *Deliverable D3.20: EPSP plug test installation report*. DOPAS project, FP7 EURATOM, no. 323273; Czech Technical University in Prague, Prague, 2016
- Šťáštka, J., The Development of Bentonite Gap Filling for High-Level Waste Disposal. In: Proceedings. Ljubljana: Nuclear Society of Slovenia, p. 908.1-908.8. ISBN 978-961-6207-36-2. 2013
- Franče J. Bentonity ve východní části Doupovských hor. Sborník geologických věd, Ložisková geologie a mineralogie 30, 43-90. 1992.
- Vašíček R., Levorová, M., Hausmannová, L., Šťáštka, J., Večerník, P., Trpkošová, D., Gondolli, J. *Deliverable 3.17 Interim results of EPSP laboratory testing*, DOPAS project FP7 EURATOM, no. 323273; Czech Technical University in Prague, Prague, January 2014
- Vašíček R., Svoboda, J., Trpkošová, D., Večerník, P., Dvořáková, M. *Deliverable 3.16 Testing plan for EPSP laboratory experiment*, DOPAS project FP7 EURATOM, no. 323273; Czech Technical University in Prague, Prague, May 2013
- Večerník, P., Záznam o provedení zkoušek pH výluhu. ÚJV Řež a. s., Husinec – Řež, January 2015
- Villar, M. V., 2007. Water retention of two natural compacted bentonites. Clays and Clay Minerals, vol. 55, No. 3, 311-322
- White, M., Doudou S., Neall, F., *Deliverable D2.1 Design Bases and Criteria*, DOPAS project FP7 EURATOM, no. 323273; Galson Sciences Limited, version 1d4 from 26 November 2013
- Záruba, J. EXPERIMENT EPSP - DOPAS - Laboratorní stanovení modulů pružnosti a přetvárnosti, pevnosti v prostém tlaku a pevnosti v příčném tahu. , Arcadis CZ a.s. (in Czech). 2015.

## 7 LIST OF ABBREVIATIONS

AEV	– Air Entry Value
B75	– Czech Ca-Mg bentonite, trade name “Bentonit 75”, produced by KERAMOST, Plc., not activated
B75_2010	– B75 delivered in 2010 (tested in 2010-2013)
B75_2013	– B75 delivered in 2013, used in DOPAS – EPSP
B75_PEL_12	– Pellets made from B75 2013 bentonite, diameter 12mm, made by commercial roller compaction technology for kaolin pellet production
B75_REC	– Pellets (crushed highly-compacted material) made from B75 2013 bentonite, non-commercial product
B75_REC_F	– A mixture of several B75 REC fractions according to Fuller’s curve (of optimal grain size distribution), here without fine particles below 0.5mm
CEC	– Cation Exchange Capacity
CEG	– Centre of Experimental Geotechnics, Faculty of Civil Engineering, Czech Technical University in Prague
DOPAS	– Full-scale Demonstration of Plugs and Seals
EGME	– Ethylene Glycol Monomethyl Ether
EPSP	– Experimental Pressure and Sealing Plug
PHM	– Physical Hydraulic Model
PIM	– Physical Interaction Model
RH	– Relative humidity
SAB65, S65	– Czech bentonite, trade name “Sabenil 65”, produced by KERAMOST, Plc., activated
SGW	– Synthetic Granitic Water
SSA	– Specific Surface Area
ÚJV	– ÚJV Řež, a. s.